

ISAC Meets SWIPT: Multi-functional Wireless Systems Integrating Sensing, Communication, and Powering

Yilong Chen, Haocheng Hua, and Jie Xu

Abstract

This paper unifies integrated sensing and communication (ISAC) and simultaneous wireless information and power transfer (SWIPT), by investigating a new multi-functional multiple-input multiple-output (MIMO) system integrating wireless sensing, communication, and powering. In this system, one multi-antenna hybrid access point (H-AP) transmits wireless signals to communicate with one multi-antenna information decoding (ID) receiver, wirelessly charge one multi-antenna energy harvesting (EH) receiver, and perform radar target sensing based on the echo signal at the same time. Under this setup, we aim to reveal the fundamental performance tradeoff limits among sensing, communication, and powering, in terms of the estimation Cramér-Rao bound (CRB), achievable communication rate, and harvested energy level, respectively. In particular, we consider two different target models for radar sensing, namely the point and extended targets, for which we are interested in estimating the target angle and the complete target response matrix, respectively. For both models, we define the achievable CRB-rate-energy (C-R-E) region and characterize its Pareto boundary by maximizing the achievable rate at the ID receiver, subject to the estimation CRB requirement for target sensing, the harvested energy requirement at the EH receiver, and the maximum transmit power constraint at the H-AP. We obtain the well-structured optimal transmit covariance solutions to the two formulated problems by applying advanced convex optimization techniques. Numerical results show the optimal C-R-E region boundary achieved by our proposed design, as compared to the benchmark schemes based on time switching and eigenmode transmission (EMT).

Part of this paper has been submitted to the IEEE International Conference on Communications (ICC), Rome, Italy, 28 May - 1 June, 2023 [1].

Y. Chen, H. Hua, and J. Xu are with the School of Science and Engineering (SSE) and the Future Network of Intelligence Institute (FNii), The Chinese University of Hong Kong (Shenzhen), Shenzhen, China (e-mail: yilongchen@link.cuhk.edu.cn, haochenghua@link.cuhk.edu.cn, xujie@cuhk.edu.cn).

J. Xu is the corresponding author.

Index Terms

Integrated sensing and communication (ISAC), simultaneous wireless information and power transfer (SWIPT), multiple-input multiple-output (MIMO), Cramér-Rao bound (CRB), achievable rate, energy harvesting, optimization.

I. INTRODUCTION

Future sixth-generation (6G) wireless networks are expected to support various new intelligent Internet-of-things (IoT) applications such as smart home, smart logistics, industrial automation, and smart healthcare [2]–[4]. Towards this end, wireless networks need to incorporate billions of low-power IoT devices and support their localization, sensing, communication, computation, and control in a sustainable manner [3]. It is projected in [4] that 6G networks need to provide the peak and user-experienced data rates of 1 Tbps and 10-100 Gbps, respectively, the localization accuracy of 1 cm indoor and 50 cm outdoor, and the battery lifetime of up to 20 years for low-power IoT devices. As a result, innovative wireless techniques are demanding to meet these stringent key performance indicators (KPIs).

On one hand, simultaneous wireless information and power transfer (SWIPT) has recently emerged as an efficient solution to provide sustainable energy supplies for massive IoT devices to enable their battery-free operation [5], by integrating the radio-frequency (RF)-based wireless power transfer (WPT) [6] and wireless communications. In SWIPT, the same wireless signals are reused for simultaneously delivering information and energy to information decoding (ID) and energy harvesting (EH) receivers, respectively. On the other hand, integrated sensing and communication (ISAC) has been recognized as an enabling technique for 6G to provide both sensing and communication functionalities [7], in which the same wireless signals can be used for not only delivering information, but also sensing surrounding targets and environments based on the echo signals [2]. With their recent advancements, we envision that future 6G networks will integrate both SWIPT and ISAC to evolve towards new multi-functional wireless systems, which can provide sensing, communication, and powering capabilities at the same time. Such multi-functional wireless systems are expected to significantly enhance the utilization efficiency of scarce spectrum resources and densely deployed base station (BS) infrastructures, and facilitate the localization and powering of massive low-power devices to support emerging IoT applications.

In the literature, there have been extensive prior works investigating the transmit optimization for SWIPT (e.g., [8]–[13]) and ISAC (e.g., [14]–[22]) independently. For instance, the authors in [8] first studied a multiple-input multiple-output (MIMO) SWIPT system with one ID receiver and one EH receiver, in which the transmit covariance at the BS was designed to optimally balance the tradeoff between the communication rate at the ID receiver versus the harvested energy level at the EH receiver. This design was then extended to the broadcast channel with multiple ID receivers and multiple EH receivers, by considering the low-complexity linear transmit beamforming [9] and the capacity-achieving dirty paper coding [10], respectively. Furthermore, other prior works investigated the SWIPT under different setups, e.g., in interference channels [11] and secrecy communications [12], or in the case with non-linear EH receivers [13]. On the other hand, for ISAC systems, the works [14] and [15] considered the basic setup with one multi-antenna BS, one multi-antenna ID receiver, and one sensing target, in which the transmit strategies at the BS were optimized to balance the communication rate versus the estimation Cramér-Rao bound (CRB) as the performance metric for target sensing. Furthermore, the authors in [16]–[18] studied the ISAC system with multiple communication users and sensing targets, in which the transmit beamforming design at the BS was optimized to balance the communication and sensing performances, in terms of the signal-to-interference-plus-noise ratio (SINR) and radar beampatterns, respectively. In addition, the work [19] developed a multi-beam transmission framework for ISAC with analog antenna arrays. Advanced multiple access techniques such as rate-splitting multiple access (RSMA) [20], [21] and non-orthogonal multiple access (NOMA) [22] were exploited for enhancing ISAC performance.

Different from these prior works investigating ISAC and SWIPT independently, this paper studies a multi-functional MIMO system unifying ISAC and SWIPT as shown in Fig. 1, in which one single multi-antenna hybrid access point (H-AP) transmits wireless signals to simultaneously deliver information to one multi-antenna ID receiver, provide energy supply to one multi-antenna EH receiver, and estimate a sensing target based on the echo signals. For such a multi-functional wireless system, how to design the transmit strategies at the multi-antenna H-AP is essential to optimize the performance tradeoffs among sensing, communication, and powering. This problem, however, is particularly challenging, due to the following reasons. First, the MIMO sensing, communication, and powering are designed based on distinct objectives and follow different principles. In particular, for MIMO radar sensing, it is known that the isotropic transmission based on an identity sample covariance matrix is beneficial in exploiting the waveform diversity

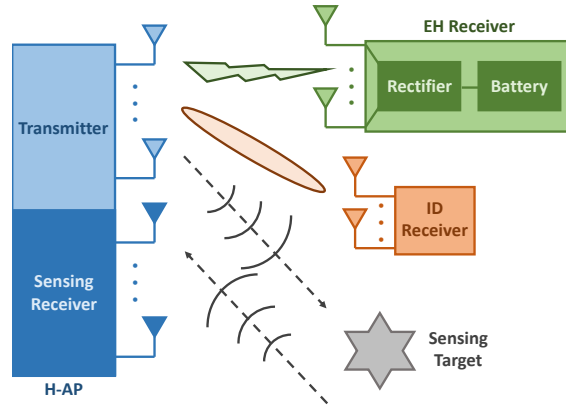


Fig. 1. A multi-functional wireless system unifying ISAC and SWIPT.

for enhancing the sensing performance [23], [24]. For point-to-point MIMO communication with perfect channel state information (CSI) at both transmitter and receiver, it is well established in [25] that the eigenmode transmission (EMT) (i.e., implementing the singular value decomposition (SVD) to decompose the MIMO communication channel) together with the water-filling power allocation over decomposed parallel subchannels is optimal for maximizing the MIMO channel capacity. For MIMO WPT with linear radio frequency (RF)-to-direct current (DC) conversion efficiency, it is shown in [8] that the strongest eigenmode transmission based on the MIMO WPT channel is optimal in maximizing the harvested energy level. Next, the MIMO sensing, communication, and powering systems deal with inter-signal-stream interference in different manners. In MIMO radar sensing, different independent probing signal beams are beneficial in reflecting target information from different perspectives. In MIMO communication, inter-signal-stream interference becomes harmful, which needs to be mitigated via proper signal processing techniques. In MIMO WPT, the inter-signal-stream interference becomes beneficial, which can be harvested to enhance the transferred energy level. Due to the above differences in sensing, communication, and powering, how to find the optimal transmission strategy for the multi-functional wireless MIMO system for balancing their performance tradeoffs is becoming an important but difficult problem. This thus motivates our study in this work.

In this paper, we consider the multi-functional MIMO system by focusing on two different target models for radar sensing, namely the point and extended targets, respectively. In the point target case, the H-AP aims to estimate the target reflection coefficient and the target angle as unknown parameters, and the target angle estimation CRB is considered as the sensing performance metric. In the extended target case, the H-AP aims to estimate the complete target

response matrix, and the corresponding matrix estimation CRB is considered. For the two cases, we aim to reveal the fundamental performance tradeoffs among sensing, communication, and powering, in terms of the estimation CRB, the achievable communication rate, and the harvested energy level, respectively. The main results of this paper are summarized as follows.

- We characterize the complete CRB-rate-energy (C-R-E) regions of the multi-functional MIMO system for the point and extended target cases, each of which is defined as the set of all C-R-E pairs that are simultaneously achievable by sensing, communication, and powering. Towards this end, we first find three vertices on the Pareto boundary of each C-R-E region corresponding to CRB minimization (C-min), rate maximization (R-max), and energy maximization (E-max), respectively, as well as three edges characterizing the optimal C-R, R-E, and C-E tradeoffs, respectively. Next, to find the remaining points on the Pareto boundary surfaces of the two C-R-E regions, we formulate two new MIMO rate maximization problems, each subject to the corresponding estimation CRB requirement for target sensing, the harvested energy requirement at the EH receiver, and the maximum transmit power constraint at the H-AP.
- We derive the well-structured optimal solutions to the two CRB-and-energy-constrained MIMO rate maximization problems by using advanced convex optimization techniques. It is shown that for the point target case, the optimal transmit covariance solution follows the EMT structure based on a composite channel matrix, together with the water-filling-like power allocation. Furthermore, the optimal transmit covariance in this case can be generally divided into two parts, one for the triple roles of communication, sensing, and powering, and the other for sensing and powering only. By contrast, for the extended target case, the optimal transmit covariance solution is obtained based on the SVD of the combined ID and EH channel matrix, which is of full rank and consists of two parts in a block diagonal form, one for the triple role of sensing, communication, and powering, and the other for dedicated sensing only.
- We provide numerical results to validate the C-R-E region boundaries achieved by the optimal solutions for the multi-functional MIMO system. For the point target case, the resultant C-R-E tradeoff is shown to highly depend on the correlations of the ID, EH, and sensing channels. For the extended target case, the resultant C-R-E tradeoff is shown to rely on the system configuration such as the number of antennas at the H-AP. Furthermore, it is shown that our proposed optimal designs significantly outperform the benchmark schemes

based on time switching, EMT over ID channel, and EMT over combined ID and EH channels.

The remainder of this paper is organized as follows. Section II presents the multi-functional wireless MIMO system models by considering the point and extended target cases, respectively. Section III characterizes the C-R-E regions of the multi-functional MIMO system for the two cases, by first finding three vertices and three edges on each Pareto boundary, and then formulating two CRB-and-energy-constrained MIMO rate maximization problems to find all remaining boundary surface points. Sections IV and V present the optimal solutions to the two formulated problems for the point and extended target cases, respectively. Section VI provides numerical results to validate the performance of our proposed designs. Finally, Section VII concludes this paper.

Notations: Boldface letters are used for vectors (lower-case) and matrices (upper-case). For a square matrix \mathbf{A} , $\text{tr}(\mathbf{A})$ and $\det(\mathbf{A})$ denote its trace and determinant, respectively, $\mathbf{A} \succeq \mathbf{0}$ means that \mathbf{A} is positive semi-definite, and $\mathbf{A} \succ \mathbf{0}$ means that \mathbf{A} is positive definite. For an arbitrary-size matrix \mathbf{A} , $\text{rank}(\mathbf{A})$, \mathbf{A}^\dagger , \mathbf{A}^T , \mathbf{A}^H , and $\mathcal{R}(\mathbf{A})$ denote its rank, conjugate, transpose, conjugate transpose, and range space, respectively. For a vector \mathbf{a} , $\|\mathbf{a}\|$ denotes its Euclidean norm. For a complex number a , $|a|$ denotes its magnitude. For a real number a , $(a)^+ \triangleq \max(a, 0)$. $\text{diag}(a_1, \dots, a_N)$ denotes a diagonal matrix whose diagonal entries are a_1, \dots, a_N . \mathbf{I}_N denotes the identity matrix with dimension $N \times N$. $\mathbb{C}^{M \times N}$, \mathbb{S}^N , and \mathbb{S}_+^N denote the spaces of $M \times N$ complex matrices, $N \times N$ Hermitian matrices, and $N \times N$ complex positive semidefinite matrices, respectively. $\mathbb{E}[\cdot]$ denotes the statistic expectation. \otimes denotes the Kronecker product. $j = \sqrt{-1}$.

II. SYSTEM MODEL

This paper considers a multi-functional MIMO system as shown in Fig. 1, which consists of one H-AP, one EH receiver, one ID receiver, and one sensing target to be estimated. The H-AP is equipped with a uniform linear array (ULA) of $M > 1$ transmit antennas and $N_S > 1$ receive antennas for sensing. The EH and ID receivers are equipped with $N_{\text{EH}} \geq 1$ and $N_{\text{ID}} \geq 1$ receive antennas, respectively.

We consider a quasi-static narrowband channel model, in which the wireless channels remain unchanged over the interested transmission block consisting of L symbols, where L is assumed to be sufficiently large. Let $\mathbf{H}_{\text{EH}} \in \mathbb{C}^{N_{\text{EH}} \times M}$ and $\mathbf{H}_{\text{ID}} \in \mathbb{C}^{N_{\text{ID}} \times M}$ denote the channel matrices from the H-AP to the EH receiver and the ID receiver, respectively. Let $\mathbf{H}_S \in \mathbb{C}^{N_S \times M}$ denote

the target response matrix from the H-AP transmitter to the sensing target to the H-AP receiver, which will be specified later for the point and extended target models, respectively. To reveal the fundamental performance upper bound limits, it is assumed that the H-AP perfectly knows the information of \mathbf{H}_{EH} and \mathbf{H}_{ID} , and the ID receiver perfectly knows \mathbf{H}_{ID} to facilitate the transmit optimization, as commonly assumed in the literature [8]–[13].

At each symbol $l \in \{1, \dots, L\}$, let $\mathbf{x}(l) \in \mathbb{C}^{M \times 1}$ denote the transmitted signal at the H-AP. The transmitted signal over the whole block is expressed as

$$\mathbf{X} = [\mathbf{x}(1), \dots, \mathbf{x}(L)] \in \mathbb{C}^{M \times L}. \quad (1)$$

Without loss of optimality, we consider the capacity-achieving Gaussian signaling, such that $\mathbf{x}(l)$'s are assumed to be circularly symmetric complex Gaussian (CSCG) random vectors with zero mean and covariance matrix $\mathbf{S} = \mathbb{E}[\mathbf{x}(l)\mathbf{x}(l)^H] \succeq \mathbf{0}$. As L is sufficiently large, the sample covariance matrix $\frac{1}{L}\mathbf{X}\mathbf{X}^H$ is approximated as the statistical covariance matrix \mathbf{S} , i.e., $\frac{1}{L}\mathbf{X}\mathbf{X}^H \approx \mathbf{S}$, which is the optimization variable to be designed.¹ Suppose that the H-AP is subject to a maximum transmit power budget P . We thus have $\mathbb{E}[\|\mathbf{x}(l)\|^2] = \text{tr}(\mathbf{S}) \leq P$.

First, we consider the radar target sensing. The echo signal received by the H-AP receiver is

$$\mathbf{Y}_S = \mathbf{H}_S \mathbf{X} + \mathbf{Z}_S, \quad (2)$$

where $\mathbf{Z}_S \in \mathbb{C}^{N_s \times L}$ denotes the additive white Gaussian noise (AWGN) at the H-AP receiver that is a CSCG random matrix with independent and identically distributed (i.i.d.) entries each with zero mean and variance σ_S^2 . The objective of sensing is to estimate the target parameters based on \mathbf{H}_S from the received echo signal \mathbf{Y}_S in (2), in which the transmitted signal \mathbf{X} is known by the H-AP. In particular, we consider two different target models, namely the point and extended targets, respectively, as specified in the following.

- **Point target case:** For the point target, the target response matrix is

$$\mathbf{H}_S = \alpha \mathbf{a}_r(\theta) \mathbf{a}_t^T(\theta) \triangleq \alpha \mathbf{A}(\theta), \quad (3)$$

where α denotes the complex reflection coefficient, θ denotes the angle of departure/arrival (AoD/AoA), and $\mathbf{a}_t(\theta) \in \mathbb{C}^{M \times 1}$ and $\mathbf{a}_r(\theta) \in \mathbb{C}^{N_s \times 1}$ denote the transmit and receive array

¹This approximation has been widely adopted in MIMO ISAC systems [15], [26].

steering vectors, respectively. By choosing the center of the ULA antennas as the reference point and assuming half-wavelength spacing between adjacent antennas, we have

$$\begin{aligned}\mathbf{a}_t(\theta) &= \left[e^{-j\frac{M-1}{2}\pi \sin(\theta)}, e^{-j\frac{M-3}{2}\pi \sin(\theta)}, \dots, e^{j\frac{M-1}{2}\pi \sin(\theta)} \right]^T, \\ \mathbf{a}_r(\theta) &= \left[e^{-j\frac{N_S-1}{2}\pi \sin(\theta)}, e^{-j\frac{N_S-3}{2}\pi \sin(\theta)}, \dots, e^{j\frac{N_S-1}{2}\pi \sin(\theta)} \right]^T.\end{aligned}\quad (4)$$

In this case, θ and α are the unknown parameters to be estimated, and the CRB for estimating θ is adopted as the sensing performance metric,² which is given by [24]

$$\text{CRB}_1(\mathbf{S}) = \frac{\sigma_S^2 \text{tr}(\mathbf{A}^H(\theta) \mathbf{A}(\theta) \mathbf{S})}{2|\alpha|^2 L \left(\text{tr}(\dot{\mathbf{A}}^H(\theta) \dot{\mathbf{A}}(\theta) \mathbf{S}) \text{tr}(\mathbf{A}^H(\theta) \mathbf{A}(\theta) \mathbf{S}) - |\text{tr}(\dot{\mathbf{A}}^H(\theta) \mathbf{A}(\theta) \mathbf{S})|^2 \right)}, \quad (5)$$

where $\dot{\mathbf{A}}(\theta) = \frac{\partial \mathbf{A}(\theta)}{\partial \theta} = \mathbf{a}_r(\theta) \dot{\mathbf{a}}_t^T(\theta) + \dot{\mathbf{a}}_r(\theta) \mathbf{a}_t^T(\theta)$. Here, $\dot{\mathbf{a}}_t(\theta)$ and $\dot{\mathbf{a}}_r(\theta)$ denote the derivatives of $\mathbf{a}_t(\theta)$ and $\mathbf{a}_r(\theta)$, respectively, i.e.,

$$\begin{aligned}\dot{\mathbf{a}}_t(\theta) &= \left[-ja_{t,1} \frac{M-1}{2} \pi \cos(\theta), -ja_{t,2} \frac{M-3}{2} \pi \cos(\theta), \dots, ja_{t,M} \frac{M-1}{2} \pi \cos(\theta) \right]^T, \\ \dot{\mathbf{a}}_r(\theta) &= \left[-ja_{r,1} \frac{N_S-1}{2} \pi \cos(\theta), -ja_{r,2} \frac{N_S-3}{2} \pi \cos(\theta), \dots, ja_{r,M} \frac{N_S-1}{2} \pi \cos(\theta) \right]^T,\end{aligned}\quad (6)$$

where $a_{t,i}$ and $a_{r,i}$ denote the i -th entries of $\mathbf{a}_t(\theta)$ and $\mathbf{a}_r(\theta)$, respectively. According to the symmetry of ULA antennas, we have $\mathbf{a}_t^H(\theta) \dot{\mathbf{a}}_t(\theta) = 0$ and $\mathbf{a}_r^H(\theta) \dot{\mathbf{a}}_r(\theta) = 0$. In the following, we define $\mathbf{A} \triangleq \mathbf{A}(\theta)$ and $\dot{\mathbf{A}} \triangleq \dot{\mathbf{A}}(\theta)$ for notational convenience.

- **Extended target case:** For the extended target, the target response matrix is [26]

$$\mathbf{H}_S = \sum_{q=1}^Q \alpha_q \mathbf{a}_r(\theta_q) \mathbf{a}_t^T(\theta_q), \quad (7)$$

where Q denotes the number of scatterers at the extended target, α_q denotes the complex reflection coefficient associated with the q -th scatterer, and θ_q denotes the AoD/AoA of the q -th scatterer. The H-AP aims to estimate the complete target response matrix \mathbf{H}_S as unknown parameters, and it is assumed that $N_S \geq M$ to ensure the estimation to be feasible. In this case, the Fisher information matrix (FIM) for estimating \mathbf{H}_S is given by $\mathbf{J} = \frac{1}{\sigma_S^2} \mathbf{X}^\dagger \mathbf{X}^T \otimes \mathbf{I}_{N_S} = \frac{L}{\sigma_S^2} \mathbf{S}^T \otimes \mathbf{I}_{N_S}$, and the corresponding CRB matrix is given by $\overline{\text{CRB}} = \mathbf{J}^{-1}$ [26]. To facilitate the performance optimization, we adopt the trace of the CRB matrix as a scalar sensing performance metric, i.e.,

$$\text{CRB}_2(\mathbf{S}) = \text{tr}(\overline{\text{CRB}}) = \frac{\sigma_S^2 N_S}{L} \text{tr}(\mathbf{S}^{-1}). \quad (8)$$

²As the target information contained in α is hard to extract, in this paper we focus on the CRB for estimating θ , similarly as in prior works [26], [27].

Next, we consider the point-to-point MIMO communication from the H-AP to the ID receiver. The received signal by the ID receiver at symbol l is given by

$$\mathbf{y}_{\text{ID}}(l) = \mathbf{H}_{\text{ID}}\mathbf{x}(l) + \mathbf{z}_{\text{ID}}(l), \quad (9)$$

where $\mathbf{z}_{\text{ID}}(l) \in \mathbb{C}^{N_{\text{ID}} \times 1}$ denotes the AWGN at the ID receiver that is a CSCG random vector with zero mean and covariance matrix $\sigma_{\text{ID}}^2 \mathbf{I}_{N_{\text{ID}}}$. With the capacity-achieving Gaussian signaling, the achievable data rate (in bps/Hz) is [25]

$$R(\mathbf{S}) = \log_2 \det \left(\mathbf{I}_{N_{\text{ID}}} + \frac{1}{\sigma_{\text{ID}}^2} \mathbf{H}_{\text{ID}} \mathbf{S} \mathbf{H}_{\text{ID}}^H \right). \quad (10)$$

Then, we consider the WPT from the H-AP to the EH receiver, where the EH receiver uses the rectifiers to convert the received RF signals into DC signals for energy harvesting. In general, the harvested DC power is monotonically increasing with respect to the received RF power. As a result, we use the received RF power (energy over a unit time duration, in Watt) at the EH receiver as the powering performance metric [5], i.e.,

$$E(\mathbf{S}) = \text{tr}(\mathbf{H}_{\text{EH}} \mathbf{S} \mathbf{H}_{\text{EH}}^H). \quad (11)$$

Our objective is to reveal the fundamental performance tradeoff among the estimation CRB (i.e., $\text{CRB}_1(\mathbf{S})$ in (5) and $\text{CRB}_2(\mathbf{S})$ in (8) for the point and extended targets, respectively), the achievable rate $R(\mathbf{S})$ in (10), and the received (unit-time) energy $E(\mathbf{S})$ in (11). Towards this end, we characterize the C-R-E region that is defined as all the C-R-E pairs simultaneously achievable in the multi-functional wireless MIMO system. For the point target case ($i = 1$) or the extended case ($i = 2$), the C-R-E region is defined as

$$\mathcal{C}_i \triangleq \{(\widehat{\text{CRB}}_i, \widehat{R}, \widehat{E}) | \widehat{\text{CRB}}_i \geq \text{CRB}_i(\mathbf{S}), \widehat{R} \leq R(\mathbf{S}), \widehat{E} \leq E(\mathbf{S}), \text{tr}(\mathbf{S}) \leq P, \mathbf{S} \succeq \mathbf{0}\}. \quad (12)$$

III. C-R-E REGION CHARACTERIZATION

This section characterizes the C-R-E region of the multi-functional MIMO system \mathcal{C}_i in (12), $i = 1, 2$, by finding its Pareto boundary, which corresponds to the set of points at which improving one performance metric will inevitably result in the deterioration of another. For instance, Fig. 2 shows the Pareto boundary of an example C-R-E region. It is observed that the complete Pareto boundary corresponds to a surface in a three-dimensional (3D) space, which is surrounded by three vertices corresponding to R-max, E-max, and C-min, respectively, as well as three edges corresponding to the optimal C-R, R-E, and C-E tradeoffs, respectively. In the following, we first explain how to find the vertices and edges in Sections III-A and III-B, respectively, and then

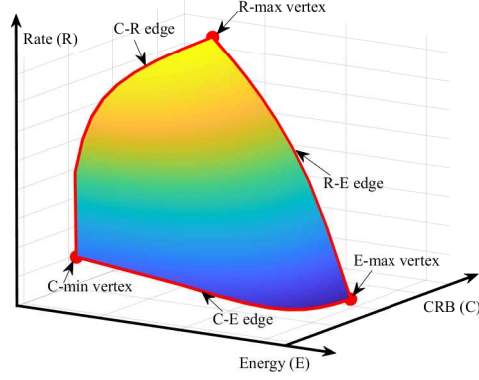


Fig. 2. The Pareto boundary of an example C-R-E region.

formulate the CRB-and-energy-constrained rate maximization problems to find the remaining interior points on the Pareto boundary surface in Section III-C.

A. Finding Three Vertices of Pareto Boundary

This subsection finds the three vertices of the C-R-E region \mathcal{C}_i , $i = 1, 2$, which correspond to R-max, E-max, and R-min, respectively. First, we consider the R-max vertex, which can be found by optimizing the transmit covariance \mathbf{S} to maximize the communication rate $R(\mathbf{S})$, i.e., $\max_{\mathbf{S} \succeq \mathbf{0}} R(\mathbf{S})$, s.t. $\text{tr}(\mathbf{S}) \leq P$. This corresponds to a sole MIMO communication system. It has been well established in [25] that the optimal transmit covariance solution to this problem, denoted by \mathbf{S}_{ID} , can be obtained by the EMT over the ID channel (i.e., performing the SVD to decompose \mathbf{H}_{ID}) together with the water-filling power allocation. Accordingly, the maximum communication rate is $R_{\text{max}} = R(\mathbf{S}_{\text{ID}})$, and the corresponding harvested energy level and estimation CRB are $E_{\text{ID}} = E(\mathbf{S}_{\text{ID}})$ and $\text{CRB}_{\text{ID},i} = \text{CRB}_i(\mathbf{S}_{\text{ID}})$ for $i \in \{1, 2\}$, respectively. As a result, the R-max vertex is obtained as $(\text{CRB}_{\text{ID},i}, R_{\text{max}}, E_{\text{ID}})$.³

Next, we consider the E-max vertex, which can be found by optimizing \mathbf{S} to maximize the harvested energy level $E(\mathbf{S})$, i.e., $\max_{\mathbf{S} \succeq \mathbf{0}} E(\mathbf{S})$, s.t. $\text{tr}(\mathbf{S}) \leq P$. This corresponds to a sole MIMO WPT system. It has been shown in [8] that the optimal solution is a rank-one matrix that can be obtained based on the strongest eigenmode transmission, denoted by $\mathbf{S}_{\text{EH}} = \sqrt{P} \mathbf{v}_{\text{max}} \mathbf{v}_{\text{max}}^H$, with \mathbf{v}_{max} being the dominant right singular vector of \mathbf{H}_{EH} . The maximum harvested energy level is hence $E_{\text{max}} = E(\mathbf{S}_{\text{EH}})$, and the corresponding communication rate and estimation CRB

³Notice that for the extended target case with $i = 2$, if \mathbf{S}_{ID} is rank-deficient, then we have $\text{CRB}_{\text{ID},2} = \frac{\sigma_s^2 N_s}{L} \text{tr}(\mathbf{S}_{\text{ID}}^{-1}) \rightarrow \infty$.

are $R_{\text{EH}} = R(\mathbf{S}_{\text{EH}})$ and $\text{CRB}_{\text{EH},i} = \text{CRB}_i(\mathbf{S}_{\text{EH}})$ for $i \in \{1, 2\}$, respectively. Thus, the E-max vertex is obtained as $(\text{CRB}_{\text{EH},i}, R_{\text{EH}}, E_{\text{max}})$.⁴

Finally, we consider the C-min vertex, which can be found by optimizing \mathbf{S} to minimize the estimation CRB $\text{CRB}_i(\mathbf{S})$ for $i \in \{1, 2\}$, i.e., $\min_{\mathbf{S} \succeq \mathbf{0}} \text{CRB}_i(\mathbf{S})$, s.t. $\text{tr}(\mathbf{S}) \leq P$. This corresponds to a sole MIMO radar sensing system. For the point target case with $i = 1$, the optimal solution $\mathbf{S}_{\text{S},1}$ has been derived in closed form in [23], where $\mathbf{S}_{\text{S},1} = \frac{P}{M} \mathbf{a}_t(\theta)^\dagger \mathbf{a}_t(\theta)^T$ holds if $N_s > M$. In this case, the minimum CRB is $\text{CRB}_{\text{min},1} = \text{CRB}_1(\mathbf{S}_{\text{S},1})$. For the extended target case with $i = 2$, the optimal solution is $\mathbf{S}_{\text{S},2} = \frac{P}{M} \mathbf{I}_M$ [15]. In this case, the minimum CRB is $\text{CRB}_{\text{min},2} = \text{CRB}_2(\mathbf{S}_{\text{S},2}) = \frac{\sigma_s^2 N_s M^2}{LP}$. With $\mathbf{S}_{\text{S},1}$ and $\mathbf{S}_{\text{S},2}$ obtained, the corresponding communication rate and harvested energy level are $R_{\text{S},i} = R(\mathbf{S}_{\text{S},i})$ and $E_{\text{S},i} = E(\mathbf{S}_{\text{S},i})$ for $i \in \{1, 2\}$, respectively. Therefore, we obtain the C-min vertex as $(\text{CRB}_{\text{min},i}, R_{\text{S},i}, E_{\text{S},i})$.

B. Finding Three Edges of Pareto Boundary

This subsection finds the three edges on the Pareto boundary of the C-R-E region \mathcal{C}_i , $i = 1, 2$, which correspond to the optimal C-R, R-E, and C-E tradeoffs, respectively. First, we find the C-R edge connecting the C-min vertex $(\text{CRB}_{\text{min},i}, R_{\text{S},i}, E_{\text{S},i})$ and the R-max vertex $(\text{CRB}_{\text{ID},i}, R_{\text{max}}, E_{\text{ID}})$. Towards this end, we optimize \mathbf{S} to maximize the communication rate $R(\mathbf{S})$ subject to a maximum estimation CRB constraint, i.e., $\max_{\mathbf{S} \succeq \mathbf{0}} R(\mathbf{S})$, s.t. $\text{CRB}_i(\mathbf{S}) \leq \text{CRB}_{\text{C-R},i}$, $\text{tr}(\mathbf{S}) \leq P$, where the CRB threshold $\text{CRB}_{\text{C-R},i}$ ranges from $\text{CRB}_{\text{min},i}$ to $\text{CRB}_{\text{ID},i}$ in order to get different C-R tradeoff points on the edge. This corresponds to the CRB-constrained rate maximization problem for the MIMO ISAC system without WPT, for which the optimal solution has been derived in [15] in semi-closed-form, denoted by $\mathbf{S}_{\text{C-R},i}$. Accordingly, let $R_{\text{C-R},i}(\text{CRB}_{\text{C-R},i}) = R(\mathbf{S}_{\text{C-R},i})$ denote the achieved communication rate with given $\text{CRB}_{\text{C-R},i}$, and $E_{\text{C-R},i}(\text{CRB}_{\text{C-R},i}) = E(\mathbf{S}_{\text{C-R},i})$ denote the corresponding harvested energy level. Then, we have the C-R edge for case $i \in \{1, 2\}$ as

$$\mathcal{C}_{\text{C-R},i} \triangleq \left\{ (\text{CRB}_{\text{C-R},i}, R_{\text{C-R},i}(\text{CRB}_{\text{C-R},i}), E_{\text{C-R},i}(\text{CRB}_{\text{C-R},i})) \mid \text{CRB}_{\text{min},i} \leq \text{CRB}_{\text{C-R},i} \leq \text{CRB}_{\text{ID},i} \right\}.$$

Next, we find the R-E edge connecting the R-max vertex $(\text{CRB}_{\text{ID},i}, R_{\text{max}}, E_{\text{ID}})$ and the E-max vertex $(\text{CRB}_{\text{EH},i}, R_{\text{EH}}, E_{\text{max}})$. Towards this end, we optimize \mathbf{S} to maximize the communication rate $R(\mathbf{S})$ subject to a minimum harvested energy constraint, i.e., $\max_{\mathbf{S} \succeq \mathbf{0}} R(\mathbf{S})$, s.t. $E(\mathbf{S}) \geq E_{\text{R-E}}$, $\text{tr}(\mathbf{S}) \leq P$, where the energy threshold $E_{\text{R-E}}$ ranges from E_{ID} to E_{max} in order to

⁴Notice that for the extended target case with $i = 2$, we always have $\text{CRB}_{\text{EH},2} = \frac{\sigma_s^2 N_s}{L} \text{tr}(\mathbf{S}_{\text{EH}}^{-1}) \rightarrow \infty$ as \mathbf{S}_{EH} is of rank one.

get different R-E tradeoff points on the edge. This corresponds to the energy-constrained rate maximization problem for the MIMO SWIPT system without radar sensing, whose optimal transmit covariance solution has been obtained in [8] as $\mathbf{S}_{\text{R-E}}$ in semi-closed-form. Accordingly, let $R_{\text{R-E}}(E_{\text{R-E}}) = R(\mathbf{S}_{\text{R-E}})$ denote the achieved communication rate, and $\text{CRB}_{\text{R-E},i}(E_{\text{R-E}}) = \text{CRB}_i(\mathbf{S}_{\text{R-E}})$ denote the corresponding estimation CRBs. Thus, the R-E tradeoff edge for case $i \in \{1, 2\}$ is given by

$$\mathcal{C}_{\text{R-E},i} \triangleq \left\{ (\text{CRB}_{\text{R-E},i}(E_{\text{R-E}}), R_{\text{R-E}}(E_{\text{R-E}}), E_{\text{R-E}}) | E_{\text{ID}} \leq E_{\text{R-E}} \leq E_{\text{max}} \right\}.$$

Finally, we find the C-E edge to connect the C-min vertex $(\text{CRB}_{\text{min},i}, R_{\text{S},i}, E_{\text{S},i})$ and the E-max vertex $(\text{CRB}_{\text{EH},i}, R_{\text{EH}}, E_{\text{max}})$. To achieve this, we optimize \mathbf{S} to maximize the harvested energy $E(\mathbf{S})$ subject to a maximum estimation CRB constraint, i.e., $\max_{\mathbf{S} \succeq \mathbf{0}} E(\mathbf{S})$, s.t. $\text{CRB}_i(\mathbf{S}) \leq \text{CRB}_{\text{C-E},i}$, $\text{tr}(\mathbf{S}) \leq P$, where the CRB threshold $\text{CRB}_{\text{C-E},i}$ ranges from $\text{CRB}_{\text{min},i}$ to $\text{CRB}_{\text{EH},i}$ in order to get different C-E tradeoff points on the edge. Notice that this corresponds to the case when there are only sensing and WPT in our integrated system. For the point target case with $i = 1$, the optimization problem can be reformulated into a convex form, as the CRB constraint $\text{CRB}_1(\mathbf{S}) \leq \text{CRB}_{\text{C-E},1}$ is equivalent to the convex semi-definite constraint
$$\begin{bmatrix} \text{tr}(\dot{\mathbf{A}}^H \dot{\mathbf{A}} \mathbf{S}) - \frac{\sigma_s^2}{2|\alpha|^2 L \text{CRB}_{\text{C-E},1}} & \text{tr}(\dot{\mathbf{A}}^H \mathbf{A} \mathbf{S})^\dagger \\ \text{tr}(\dot{\mathbf{A}}^H \mathbf{A} \mathbf{S}) & \text{tr}(\mathbf{A}^H \mathbf{A} \mathbf{S}) \end{bmatrix} \succeq \mathbf{0}$$
 based on the Schur complement [26]. Therefore, the optimal solution $\mathbf{S}_{\text{C-E},1}$ in this case can be found by standard convex optimization techniques [28].⁵ For the extended target case with $i = 2$, the semi-closed-form optimal solution $\mathbf{S}_{\text{C-E},2}$ can be obtained similarly as in [29]. Let $E_{\text{C-E},i}(\text{CRB}_{\text{C-E},i}) = E(\mathbf{S}_{\text{C-E},i})$ denote the achieved harvested energy level, and $R_{\text{C-E},i}(\text{CRB}_{\text{C-E},i}) = R(\mathbf{S}_{\text{C-E},i})$ denote the corresponding communication rate. Accordingly, the C-E tradeoff edge for case $i \in \{1, 2\}$ is expressed as

$$\mathcal{C}_{\text{C-E},i} \triangleq \left\{ (\text{CRB}_{\text{C-E},i}, R_{\text{C-E},i}(\text{CRB}_{\text{C-E},i}), E_{\text{C-E},i}(\text{CRB}_{\text{C-E},i})) | \text{CRB}_{\text{min},i} \leq \text{CRB}_{\text{C-E},i} \leq \text{CRB}_{\text{EH},i} \right\}.$$

C. Characterizing Complete Pareto Boundary Surface

With the vertices and edges obtained, it remains to find the interior points on the Pareto boundary surface to characterize the complete C-R-E region \mathcal{C}_i for case $i \in \{1, 2\}$. Towards this end, we optimize the transmit covariance \mathbf{S} to maximize the communication rate $R(\mathbf{S})$ in (10), subject to a maximum estimation CRB constraint Γ_{S} and a minimum harvested energy

⁵Note that we can obtain a well-structured optimal solution to this problem by the Lagrangian duality method. However, we omit the derivation here as it will be similar to that for the more general problem (P1) in Section IV.

constraint Γ_{EH} . Mathematically, the CRB-and-energy-constrained rate maximization problem for case $i \in \{1, 2\}$ is formulated as

$$(\text{P}i) : \max_{\mathbf{S} \succeq \mathbf{0}} \log_2 \det \left(\mathbf{I}_{N_{\text{ID}}} + \frac{1}{\sigma_{\text{ID}}^2} \mathbf{H}_{\text{ID}} \mathbf{S} \mathbf{H}_{\text{ID}}^H \right) \quad (13a)$$

$$\text{s.t. } \text{tr}(\mathbf{H}_{\text{EH}} \mathbf{S} \mathbf{H}_{\text{EH}}^H) \geq \Gamma_{\text{EH}} \quad (13b)$$

$$\text{CRB}_i(\mathbf{S}) \leq \Gamma_{\text{S}} \quad (13c)$$

$$\text{tr}(\mathbf{S}) \leq P. \quad (13d)$$

By exhausting Γ_{EH} and Γ_{S} enclosed by the projection of the three edges on the C-E plane, we can obtain all the Pareto boundary surface points. In particular, let $R_i^*(\Gamma_{\text{EH}}, \Gamma_{\text{S}})$ denote the optimal value of problem (Pi) with given Γ_{EH} and Γ_{S} . Then we have one Pareto boundary point of the C-R-E region \mathcal{C}_i as $(\Gamma_{\text{S}}, R_i^*(\Gamma_{\text{EH}}, \Gamma_{\text{S}}), \Gamma_{\text{EH}})$.

In Sections IV and V, we focus on solving problems (P1) and (P2) for the point and extended target cases, respectively.

IV. OPTIMAL SOLUTION TO PROBLEM (P1) WITH POINT TARGET

In this section, we present the optimal solution to problem (P1) in the point target case. Notice that (P1) is not convex due to the estimation CRB constraint in (13c) for $i = 1$. Fortunately, based on the Schur complement, constraint (13c) for $i = 1$ is equivalent to

$$\begin{bmatrix} \text{tr}(\dot{\mathbf{A}}^H \dot{\mathbf{A}} \mathbf{S}) - \frac{1}{\Gamma_{\text{S},1}} & \text{tr}(\dot{\mathbf{A}}^H \mathbf{A} \mathbf{S})^\dagger \\ \text{tr}(\dot{\mathbf{A}}^H \mathbf{A} \mathbf{S}) & \text{tr}(\mathbf{A}^H \mathbf{A} \mathbf{S}) \end{bmatrix} \succeq \mathbf{0}, \quad (14)$$

where $\Gamma_{\text{S},1} \triangleq \frac{2|\alpha|^2 L}{\sigma_{\text{S}}^2} \Gamma_{\text{S}}$. Therefore, by replacing constraint (13c) as that in (14), (P1) is reformulated into a convex form, which can be optimally solved by using the Lagrangian duality method.

Let $\lambda \geq 0$, $\nu \geq 0$, and $\mathbf{Z} \triangleq \begin{bmatrix} z_1 & z_2 \\ z_2^\dagger & z_3 \end{bmatrix} \succeq \mathbf{0}$ denote the dual variables associated with the constraints in (13b), (13d), and (14), respectively. The Lagrangian of problem (P1) is given by

$$\begin{aligned} \mathcal{L}(\mathbf{S}, \lambda, \nu, \mathbf{Z}) &= \log_2 \det \left(\mathbf{I}_{N_{\text{ID}}} + \frac{1}{\sigma_{\text{ID}}^2} \mathbf{H}_{\text{ID}} \mathbf{S} \mathbf{H}_{\text{ID}}^H \right) + \lambda (\text{tr}(\mathbf{H}_{\text{EH}} \mathbf{S} \mathbf{H}_{\text{EH}}^H) - \Gamma_{\text{EH}}) + \nu (P - \text{tr}(\mathbf{S})) \\ &\quad + \text{tr} \left(\mathbf{Z} \begin{bmatrix} \text{tr}(\dot{\mathbf{A}}^H \dot{\mathbf{A}} \mathbf{S}) - \frac{1}{\Gamma_{\text{S},1}} & \text{tr}(\dot{\mathbf{A}}^H \mathbf{A} \mathbf{S})^\dagger \\ \text{tr}(\dot{\mathbf{A}}^H \mathbf{A} \mathbf{S}) & \text{tr}(\mathbf{A}^H \mathbf{A} \mathbf{S}) \end{bmatrix} \right) \\ &= \log_2 \det \left(\mathbf{I}_{N_{\text{ID}}} + \frac{1}{\sigma_{\text{ID}}^2} \mathbf{H}_{\text{ID}} \mathbf{S} \mathbf{H}_{\text{ID}}^H \right) - \text{tr}(\mathbf{D} \mathbf{S}) - \lambda \Gamma_{\text{EH}} + \nu P - \frac{z_1}{\Gamma_{\text{S},1}}, \end{aligned} \quad (15)$$

where $\mathbf{D} \triangleq \nu \mathbf{I}_M - \lambda \mathbf{H}_{\text{EH}}^H \mathbf{H}_{\text{EH}} - z_1 \dot{\mathbf{A}}^H \dot{\mathbf{A}} - z_2 \dot{\mathbf{A}}^H \mathbf{A} - z_2^\dagger \mathbf{A}^H \dot{\mathbf{A}} - z_3 \mathbf{A}^H \mathbf{A}$. Note that $\dot{\mathbf{A}} = \mathbf{a}_r \dot{\mathbf{a}}_t^T + \dot{\mathbf{a}}_r \mathbf{a}_t^T$ and $\mathbf{a}_t^H \dot{\mathbf{a}}_t = \mathbf{a}_r^H \dot{\mathbf{a}}_r = 0$. As a result, it follows that $\mathbf{D} = \nu \mathbf{I}_M - \lambda \mathbf{H}_{\text{EH}}^H \mathbf{H}_{\text{EH}} - (z_1 \dot{\mathbf{a}}_t^\dagger \dot{\mathbf{a}}_t^T + z_2 \dot{\mathbf{a}}_t^\dagger \mathbf{a}_t^T + z_2^\dagger \mathbf{a}_t^\dagger \dot{\mathbf{a}}_t^T + z_3 \mathbf{a}_t^\dagger \mathbf{a}_t^T) \|\mathbf{a}_r\|^2 - z_1 \mathbf{a}_t^\dagger \mathbf{a}_t^T \|\dot{\mathbf{a}}_r\|^2$.

Accordingly, the dual function of problem (P1) is defined as

$$g(\lambda, \nu, \mathbf{Z}) = \max_{\mathbf{S} \succeq \mathbf{0}} \mathcal{L}(\mathbf{S}, \lambda, \nu, \mathbf{Z}). \quad (16)$$

We have the following lemma, which can be verified similarly as in [15, Lemma 1].

Lemma 1: In order for the dual function $g(\lambda, \nu, \mathbf{Z})$ to be bounded from above, it must hold that

$$\mathbf{D} \succeq \mathbf{0} \text{ and } \mathcal{R}(\mathbf{H}_{\text{ID}}^H) \subseteq \mathcal{R}(\mathbf{D}). \quad (17)$$

Based on Lemma 1, the dual problem of (P1) is defined as

$$(\text{D1}) : \min_{\lambda \geq 0, \nu \geq 0, \mathbf{Z} \succeq \mathbf{0}} g(\lambda, \nu, \mathbf{Z}), \text{ s.t. (17)}. \quad (18)$$

Since problem (P1) is reformulated into a convex form and satisfies the Slater's condition, strong duality holds between (P1) and its dual problem (D1) [30]. Therefore, we can solve (P1) by equivalently solving (D1). In the following, we first obtain the dual function $g(\lambda, \nu, \mathbf{Z})$ with given dual variables, and then search over $\lambda \geq 0$, $\nu \geq 0$, and $\mathbf{Z} \succeq \mathbf{0}$ to minimize $g(\lambda, \nu, \mathbf{Z})$.

A. Finding Dual Function $g(\lambda, \nu, \mathbf{Z})$ of Problem (P1)

First, we find the dual function $g(\lambda, \nu, \mathbf{Z})$ in (16) under given $\lambda \geq 0$, $\nu \geq 0$, and $\mathbf{Z} \succeq \mathbf{0}$ satisfying (17). By dropping the constant terms $-\lambda \Gamma_{\text{EH}} + \nu P - \frac{z_1}{\Gamma_{\text{S},1}}$, the problem in (16) is equivalent to

$$\max_{\mathbf{S} \succeq \mathbf{0}} \log_2 \det \left(\mathbf{I}_{N_{\text{ID}}} + \frac{1}{\sigma_{\text{ID}}^2} \mathbf{H}_{\text{ID}} \mathbf{S} \mathbf{H}_{\text{ID}}^H \right) - \text{tr}(\mathbf{D} \mathbf{S}). \quad (19)$$

Suppose that $\text{rank}(\mathbf{D}) = r_p$, the eigenvalue decomposition (EVD) of \mathbf{D} can be expressed as

$$\mathbf{D} = \begin{bmatrix} \mathbf{Q}^{\overline{\text{null}}} & \mathbf{Q}^{\text{null}} \end{bmatrix} \begin{bmatrix} \Sigma^{\overline{\text{null}}} & \mathbf{0} \\ \mathbf{0} & \mathbf{0} \end{bmatrix} \begin{bmatrix} \mathbf{Q}^{\overline{\text{null}H}} \\ \mathbf{Q}^{\text{null}H} \end{bmatrix}, \quad (20)$$

where $\Sigma^{\overline{\text{null}}} = \text{diag}(\sigma_{p,1}, \dots, \sigma_{p,r_p})$, and $\mathbf{Q}^{\overline{\text{null}}} \in \mathbb{C}^{M \times r_p}$ and $\mathbf{Q}^{\text{null}} \in \mathbb{C}^{M \times (M-r_p)}$ denote the eigenvectors corresponding to the r_p non-zero eigenvalues $\sigma_{p,1}, \dots, \sigma_{p,r_p}$, and the remaining $M - r_p$ zero eigenvalues, respectively. Without loss of generality, we express \mathbf{S} as

$$\begin{aligned} \mathbf{S} &= \begin{bmatrix} \mathbf{Q}^{\overline{\text{null}}} & \mathbf{Q}^{\text{null}} \end{bmatrix} \begin{bmatrix} \mathbf{S}_{11} & \mathbf{C} \\ \mathbf{C}^H & \mathbf{S}_{00} \end{bmatrix} \begin{bmatrix} \mathbf{Q}^{\overline{\text{null}H}} \\ \mathbf{Q}^{\text{null}H} \end{bmatrix} \\ &= \mathbf{Q}^{\overline{\text{null}}} \mathbf{S}_{11} \mathbf{Q}^{\overline{\text{null}H}} + \mathbf{Q}^{\overline{\text{null}}} \mathbf{C} \mathbf{Q}^{\text{null}H} + \mathbf{Q}^{\text{null}} \mathbf{C}^H \mathbf{Q}^{\overline{\text{null}H}} + \mathbf{Q}^{\text{null}} \mathbf{S}_{00} \mathbf{Q}^{\text{null}H}, \end{aligned} \quad (21)$$

where $\mathbf{S}_{11} \in \mathbb{S}^{r_p}$, $\mathbf{S}_{00} \in \mathbb{S}^{M-r_p}$, and $\mathbf{C} \in \mathbb{C}^{r_p \times (M-r_p)}$ are variables to be optimized. Supposing that $\text{rank}(\mathbf{H}_{\text{ID}} \mathbf{Q}^{\text{null}} (\boldsymbol{\Sigma}^{\text{null}})^{-\frac{1}{2}}) = \tilde{r}_p$, we have the truncated SVD as $\mathbf{H}_{\text{ID}} \mathbf{Q}^{\text{null}} (\boldsymbol{\Sigma}^{\text{null}})^{-\frac{1}{2}} = \mathbf{U}_p \boldsymbol{\Lambda}_p \mathbf{V}_p^H$, where $\mathbf{U}_p \in \mathbb{C}^{N_{\text{ID}} \times \tilde{r}_p}$, $\mathbf{V}_p \in \mathbb{C}^{r_p \times \tilde{r}_p}$, and $\boldsymbol{\Lambda}_p = \text{diag}(\lambda_{p,1}, \dots, \lambda_{p,\tilde{r}_p})$. Then we have the following proposition.

Proposition 1: The optimal solution to problem (19) is given by

$$\mathbf{S}^* = \begin{bmatrix} \mathbf{Q}^{\text{null}} & \mathbf{Q}^{\text{null}} \end{bmatrix} \begin{bmatrix} \mathbf{S}_{11}^* & \mathbf{C}^* \\ \mathbf{C}^{*H} & \mathbf{S}_{00}^* \end{bmatrix} \begin{bmatrix} \mathbf{Q}^{\text{null}H} \\ \mathbf{Q}^{\text{null}H} \end{bmatrix}, \quad (22)$$

where

$$\mathbf{S}_{11}^* = (\boldsymbol{\Sigma}^{\text{null}})^{-\frac{1}{2}} \mathbf{V}_p \text{diag}(\tilde{p}_1, \dots, \tilde{p}_{\tilde{r}_p}) \mathbf{V}_p^H (\boldsymbol{\Sigma}^{\text{null}})^{-\frac{1}{2}}, \quad (23)$$

with

$$\tilde{p}_k = \left(\frac{1}{\ln 2} - \frac{\sigma_{\text{ID}}^2}{\lambda_{p,k}^2} \right)^+, \forall k \in \{1, \dots, \tilde{r}_p\}, \quad (24)$$

and \mathbf{C}^* and $\mathbf{S}_{00}^* \succeq \mathbf{0}$ can be chosen arbitrarily such that $\mathbf{S}^* \succeq \mathbf{0}$.⁶

Proof: See Appendix A.

B. Solving Dual Problem (D1)

Next, we solve the dual problem (D1), which is convex but not necessarily differentiable. Therefore, we can solve (D1) by applying subgradient-based methods such as the ellipsoid method [30]. First, for the objective function $g(\lambda, \nu, \mathbf{Z})$, the subgradient at $(\lambda, \nu, z_1, z_2, z_3)$ is $[\text{tr}(\mathbf{H}_{\text{EH}}^H \mathbf{H}_{\text{EH}} \mathbf{S}^*) - \Gamma_{\text{EH}}, P - \text{tr}(\mathbf{S}^*), \text{tr}(\dot{\mathbf{A}}^H \dot{\mathbf{A}} \mathbf{S}^*) - \frac{1}{\Gamma_{s,1}}, \text{tr}(\dot{\mathbf{A}}^H \mathbf{A} \mathbf{S}^* + \mathbf{A}^H \dot{\mathbf{A}} \mathbf{S}^*) + j \text{tr}(\dot{\mathbf{A}}^H \mathbf{A} \mathbf{S}^* - \mathbf{A}^H \dot{\mathbf{A}} \mathbf{S}^*), \text{tr}(\mathbf{A}^H \mathbf{A} \mathbf{S}^*)]^T$. Then, let \mathbf{q}_1 denote the eigenvector corresponding to the minimum eigenvalue of \mathbf{D} . Since constraint $\mathbf{D} \succeq \mathbf{0}$ is equivalent to $\mathbf{q}_1^H \mathbf{D} \mathbf{q}_1 \geq 0$, the subgradient of constraint $\mathbf{D} \succeq \mathbf{0}$ at $(\lambda, \nu, z_1, z_2, z_3)$ is $[\mathbf{q}_1^H \mathbf{H}_{\text{EH}}^H \mathbf{H}_{\text{EH}} \mathbf{q}_1, -1, \mathbf{q}_1^H \dot{\mathbf{A}}^H \dot{\mathbf{A}} \mathbf{q}_1, \mathbf{q}_1^H (\dot{\mathbf{A}}^H \mathbf{A} + \mathbf{A}^H \dot{\mathbf{A}}) \mathbf{q}_1 + j \mathbf{q}_1^H (\dot{\mathbf{A}}^H \mathbf{A} - \mathbf{A}^H \dot{\mathbf{A}}) \mathbf{q}_1, \mathbf{q}_1^H \mathbf{A}^H \mathbf{A} \mathbf{q}_1]^T$. Furthermore, let $\mathbf{q}_2 = [q_{2,1}, q_{2,2}]^T$ denote the eigenvector corresponding to the minimum eigenvalue of \mathbf{Z} . The subgradient of constraint $\mathbf{Z} \succeq \mathbf{0}$ at $(\lambda, \nu, z_1, z_2, z_3)$ is $[0, 0, -|q_{2,1}|^2, -(q_{2,1}^\dagger q_{2,2} + q_{2,2}^\dagger q_{2,1}) - j(q_{2,1}^\dagger q_{2,2} - q_{2,2}^\dagger q_{2,1}), -|q_{2,2}|^2]^T$. With these derived subgradients, the ellipsoid method can be implemented efficiently, based on which we can obtain the optimal dual solution to (D1) as λ^* , ν^* , and \mathbf{Z}^* .

⁶Note that \mathbf{C}^* and \mathbf{S}_{00}^* are non-unique here, and as a result, we need an additional step to determine them for solving the primal problem (P1) later. Here, we can simply choose $\mathbf{C}^* = \mathbf{0}$ and $\mathbf{S}_{00}^* = \mathbf{0}$ for obtaining the dual function $g(\lambda, \nu, \mathbf{Z})$ only.

C. Optimal Solution to Primal Problem (P1)

Now, we present the optimal solution to the primal problem (P1). With the optimal dual variables λ^* , ν^* , and \mathbf{Z}^* at hand, the corresponding unique optimal solution \mathbf{S}_{11}^* to problem (19) can be directly used for constructing the optimal primal solution to (P1), denoted by $\mathbf{S}_{11}^{\text{opt}}$. However, as indicated in Section IV-A, the optimal solutions of \mathbf{C}^* and \mathbf{S}_{00}^* to (19) are not unique. As a result, with given $\mathbf{S}_{11}^{\text{opt}}$, we need to find the optimal solutions of \mathbf{C} and \mathbf{S}_{00} , denoted by \mathbf{C}^{opt} and $\mathbf{S}_{00}^{\text{opt}}$, by solving one additional feasibility problem. We have the following proposition.

Proposition 2: The optimal solution to problem (P1) is

$$\mathbf{S}^{\text{opt},1} = \begin{bmatrix} \mathbf{Q}^{\text{null}} & \mathbf{Q}^{\text{null}} \end{bmatrix} \begin{bmatrix} \mathbf{S}_{11}^{\text{opt}} & \mathbf{C}^{\text{opt}} \\ \mathbf{C}^{\text{opt}H} & \mathbf{S}_{00}^{\text{opt}} \end{bmatrix} \begin{bmatrix} \mathbf{Q}^{\text{null}H} \\ \mathbf{Q}^{\text{null}H} \end{bmatrix}, \quad (25)$$

where $\mathbf{S}_{11}^{\text{opt}}$ is given by (23) based on λ^* , ν^* , and \mathbf{Z}^* , and \mathbf{C}^{opt} and $\mathbf{S}_{00}^{\text{opt}}$ are obtained by solving the following feasibility problem.

find \mathbf{C} and \mathbf{S}_{00}

s.t. (13b), (13d), and (14) (26)

$$\mathbf{S} = \mathbf{Q}^{\text{null}} \mathbf{S}_{11}^{\text{opt}} \mathbf{Q}^{\text{null}H} + \mathbf{Q}^{\text{null}} \mathbf{C} \mathbf{Q}^{\text{null}H} + \mathbf{Q}^{\text{null}} \mathbf{C}^H \mathbf{Q}^{\text{null}H} + \mathbf{Q}^{\text{null}} \mathbf{S}_{00} \mathbf{Q}^{\text{null}H}.$$

Remark 1: Based on Proposition 2, we have the following interesting observations on the optimal transmit covariance solution $\mathbf{S}^{\text{opt},1}$ for the point target case. First, $\mathbf{S}^{\text{opt},1}$ follows the EMT structure based on the composite channel \mathbf{D} consisting of ID, EH, and sensing channels (see (20)), together with the water-filling-like power allocation (see (24)). Next, it is observed that $\mathbf{S}^{\text{opt},1}$ is divided into two parts, i.e., $\mathbf{S}_{11}^{\text{opt}}$ for the triple roles of communication, sensing, and powering; and \mathbf{C}^{opt} and $\mathbf{S}_{00}^{\text{opt}}$ for sensing and powering only. Notice that based on extensive simulations, we find that with randomly generated channels, it follows that $\mathbf{D} \succ \mathbf{0}$ and $\mathbf{S}^{\text{opt},1} = \mathbf{Q}^{\text{null}} \mathbf{S}_{11}^{\text{opt}} \mathbf{Q}^{\text{null}H}$, i.e., only $\mathbf{S}_{11}^{\text{opt}}$ is needed; by contrast, in some special cases (e.g., \mathbf{H}_{ID} and \mathbf{H}_{EH} being orthogonal to \mathbf{A}), it could happen that \mathbf{D} is rank-deficient, and thus \mathbf{C}^{opt} and $\mathbf{S}_{00}^{\text{opt}}$ are also needed.

V. OPTIMAL SOLUTION TO PROBLEM (P2) WITH EXTENDED TARGET

In this section, we address problem (P2) in the extended target case. For convenience, we rewrite the constraint in (13c) for $i = 2$ as

$$\text{tr}(\mathbf{S}^{-1}) \leq \Gamma_{\text{S},2}, \quad (27)$$

where $\Gamma_{S,2} \triangleq \frac{L}{\sigma_S^2 N_S} \Gamma_S$. Notice that (P2) is convex and thus can be solved by using standard convex optimization techniques [28]. In the following, we develop an efficient algorithm to obtain a well-structural solution of \mathbf{S} to (P2).

A. Optimal Solution to (P2) Based on Problem Reformulation

This subsection finds the optimal solution to problem (P2) based on problem reformulation. First, we define $\mathbf{H} \triangleq [\mathbf{H}_{\text{ID}}^T \ \mathbf{H}_{\text{EH}}^T]^T \in \mathbb{C}^{(N_{\text{ID}}+N_{\text{EH}}) \times M}$, which corresponds to the combined ID and EH channel matrix with $\text{rank}(\mathbf{H}) = r$. The SVD of \mathbf{H} is expressed as

$$\mathbf{H} = \begin{bmatrix} \mathbf{U}^{\overline{\text{null}}} & \mathbf{U}^{\text{null}} \end{bmatrix} \begin{bmatrix} \mathbf{\Lambda}^{\overline{\text{null}}} & \mathbf{0} \\ \mathbf{0} & \mathbf{0} \end{bmatrix} \begin{bmatrix} \mathbf{V}^{\overline{\text{null}}}{}^H \\ \mathbf{V}^{\text{null}}{}^H \end{bmatrix}, \quad (28)$$

where $\mathbf{\Lambda}^{\overline{\text{null}}} = \text{diag}(\lambda_1, \dots, \lambda_r)$, and $\mathbf{V}^{\overline{\text{null}}} \in \mathbb{C}^{M \times r}$ and $\mathbf{V}^{\text{null}} \in \mathbb{C}^{M \times (M-r)}$ denote the right singular vectors corresponding to the r non-zero singular values and the $M - r$ zero singular values of \mathbf{H} , respectively. Without loss of generality, we express \mathbf{S} as

$$\begin{aligned} \mathbf{S} &= \begin{bmatrix} \mathbf{V}^{\overline{\text{null}}} & \mathbf{V}^{\text{null}} \end{bmatrix} \begin{bmatrix} \mathbf{S}_1 & \mathbf{B} \\ \mathbf{B}^H & \mathbf{S}_0 \end{bmatrix} \begin{bmatrix} \mathbf{V}^{\overline{\text{null}}}{}^H \\ \mathbf{V}^{\text{null}}{}^H \end{bmatrix} \\ &= \mathbf{V}^{\overline{\text{null}}} \mathbf{S}_1 \mathbf{V}^{\overline{\text{null}}}{}^H + \mathbf{V}^{\overline{\text{null}}} \mathbf{B} \mathbf{V}^{\text{null}}{}^H + \mathbf{V}^{\text{null}} \mathbf{B}^H \mathbf{V}^{\overline{\text{null}}}{}^H + \mathbf{V}^{\text{null}} \mathbf{S}_0 \mathbf{V}^{\text{null}}{}^H, \end{aligned} \quad (29)$$

where $\mathbf{S}_1 \in \mathbb{S}^r$, $\mathbf{S}_0 \in \mathbb{S}^{M-r}$, and $\mathbf{B} \in \mathbb{C}^{r \times (M-r)}$ are variables to be optimized.

Since $\mathbf{V}^{\overline{\text{null}}}{}^H \mathbf{V}^{\text{null}} = \mathbf{0}$, we have $\mathbf{H} \mathbf{V}^{\text{null}} = \mathbf{0}$, which implies that $\mathbf{H}_{\text{ID}} \mathbf{V}^{\text{null}} = \mathbf{0}$ and $\mathbf{H}_{\text{EH}} \mathbf{V}^{\text{null}} = \mathbf{0}$. Substituting (29), problem (P2) is re-expressed as

$$(\text{P2.1}) : \max_{\mathbf{S}_1, \mathbf{S}_0, \mathbf{B}} \log_2 \det \left(\mathbf{I}_{N_{\text{ID}}} + \frac{1}{\sigma_{\text{ID}}^2} \mathbf{H}_{\text{ID}} \mathbf{V}^{\overline{\text{null}}} \mathbf{S}_1 \mathbf{V}^{\overline{\text{null}}}{}^H \mathbf{H}_{\text{ID}}^H \right) \quad (30a)$$

$$\text{s.t. } \text{tr}(\mathbf{H}_{\text{EH}} \mathbf{V}^{\overline{\text{null}}} \mathbf{S}_1 \mathbf{V}^{\overline{\text{null}}}{}^H \mathbf{H}_{\text{EH}}^H) \geq \Gamma_{\text{EH}} \quad (30b)$$

$$\text{tr} \left(\begin{bmatrix} \mathbf{S}_1 & \mathbf{B} \\ \mathbf{B}^H & \mathbf{S}_0 \end{bmatrix}^{-1} \right) \leq \Gamma_{S,2} \quad (30c)$$

$$\text{tr}(\mathbf{S}_1) + \text{tr}(\mathbf{S}_0) \leq P \quad (30d)$$

$$\begin{bmatrix} \mathbf{S}_1 & \mathbf{B} \\ \mathbf{B}^H & \mathbf{S}_0 \end{bmatrix} \succeq \mathbf{0}. \quad (30e)$$

We have the following proposition.

Proposition 3: At the optimal solution of problem (P2.1), it holds that $\mathbf{B} = \mathbf{0}$.

Proof: See Appendix B.

According to Proposition 3, the optimal solution to problem (P2) or (P2.1) has the form of $\mathbf{S} = \mathbf{V}^{\overline{\text{null}}} \mathbf{S}_1 \mathbf{V}^{\overline{\text{null}}^H} + \mathbf{V}^{\text{null}} \mathbf{S}_0 \mathbf{V}^{\text{null}^H}$. Accordingly, (P2.1) is equivalently reformulated as

$$(P2.2) : \max_{\mathbf{S}_1, \mathbf{S}_0} \log_2 \det \left(\mathbf{I}_{N_{\text{ID}}} + \frac{1}{\sigma_{\text{ID}}^2} \widetilde{\mathbf{H}}_{\text{ID}} \mathbf{S}_1 \widetilde{\mathbf{H}}_{\text{ID}}^H \right) \quad (31a)$$

$$\text{s.t. } \text{tr}(\widetilde{\mathbf{H}}_{\text{EH}} \mathbf{S}_1 \widetilde{\mathbf{H}}_{\text{EH}}^H) \geq \Gamma_{\text{EH}} \quad (31b)$$

$$\text{tr}(\mathbf{S}_1^{-1}) + \text{tr}(\mathbf{S}_0^{-1}) \leq \Gamma_{\text{S},2} \quad (31c)$$

$$\text{tr}(\mathbf{S}_1) + \text{tr}(\mathbf{S}_0) \leq P \quad (31d)$$

$$\mathbf{S}_1 \succeq \mathbf{0} \text{ and } \mathbf{S}_0 \succeq \mathbf{0}, \quad (31e)$$

where $\widetilde{\mathbf{H}}_{\text{ID}} \triangleq \mathbf{H}_{\text{ID}} \mathbf{V}^{\overline{\text{null}}}$ and $\widetilde{\mathbf{H}}_{\text{EH}} \triangleq \mathbf{H}_{\text{EH}} \mathbf{V}^{\overline{\text{null}}}$ are defined as the projection of the ID and EH channels on the range space of the combined channel \mathbf{H} , respectively. We have the following proposition.

Proposition 4: The optimal solution of \mathbf{S}_0 to problem (P2.2) has the form of $\mathbf{S}_0 = p_0 \mathbf{I}_{M-r}$.

Proof: See Appendix C.

From Proposition 4, the optimization of matrix \mathbf{S}_0 in problem (P2.2) can be simplified as the optimization of a scalar variable p_0 . Thus, (P2.2) is further reformulated as

$$(P2.3) : \max_{\mathbf{S}_1 \succeq \mathbf{0}, p_0 \geq 0} \log_2 \det \left(\mathbf{I}_{N_{\text{ID}}} + \frac{1}{\sigma_{\text{ID}}^2} \widetilde{\mathbf{H}}_{\text{ID}} \mathbf{S}_1 \widetilde{\mathbf{H}}_{\text{ID}}^H \right) \quad (32a)$$

$$\text{s.t. } \text{tr}(\widetilde{\mathbf{H}}_{\text{EH}} \mathbf{S}_1 \widetilde{\mathbf{H}}_{\text{EH}}^H) \geq \Gamma_{\text{EH}} \quad (32b)$$

$$\text{tr}(\mathbf{S}_1^{-1}) + (M-r) \frac{1}{p_0} \leq \Gamma_{\text{S},2} \quad (32c)$$

$$\text{tr}(\mathbf{S}_1) + (M-r)p_0 \leq P. \quad (32d)$$

Note that problem (P2.3) is also convex, and thus we solve it by using standard convex solvers such as CVX [28]. Let $\mathbf{S}_1^{\text{opt}}$ and p_0^{opt} denote the optimal solution to (P2.3). Then the optimal solution to problem (P2) is given by

$$\mathbf{S}^{\text{opt},2} = \mathbf{V}^{\overline{\text{null}}} \mathbf{S}_1^{\text{opt}} \mathbf{V}^{\overline{\text{null}}^H} + p_0^{\text{opt}} \mathbf{V}^{\text{null}} \mathbf{V}^{\text{null}^H}. \quad (33)$$

Remark 2: Based on (33), the optimal transmit covariance solution $\mathbf{S}^{\text{opt},2}$ for the extended target case is different from $\mathbf{S}^{\text{opt},1}$ for the point target case, in the following aspects. First, different from $\mathbf{S}^{\text{opt},1}$ that is obtained based on the SVD of composite channel matrix \mathbf{D} , $\mathbf{S}^{\text{opt},2}$ is obtained based on that of the combined ID and EH channels $\mathbf{H} = [\mathbf{H}_{\text{ID}}^T \mathbf{H}_{\text{EH}}^T]^T$. Accordingly, $\mathbf{S}^{\text{opt},2}$ is divided into two parts, i.e., $\mathbf{V}^{\overline{\text{null}}} \mathbf{S}_1^{\text{opt}} \mathbf{V}^{\overline{\text{null}}^H}$ for the triple roles in communication,

powering, and sensing, and $p_0^{\text{opt}} \mathbf{V}^{\text{null}} \mathbf{V}^{\text{null}H}$ for sensing only. Here, the second part is different from \mathbf{C}^{opt} and $\mathbf{S}_{00}^{\text{opt}}$ for both sensing and powering in the point target case. Next, we have $\mathbf{S}_1^{\text{opt}}$ in (33) being a general positive semidefinite matrix for the extended target case, which is different from $\mathbf{S}_{11}^{\text{opt}}$ that is diagonal for the point target case. Furthermore, we have the dedicated sensing signal part $p_0^{\text{opt}} \mathbf{V}^{\text{null}} \mathbf{V}^{\text{null}H}$ in (33), which is always needed for the case with $M > r$. This is different from \mathbf{C}^{opt} and $\mathbf{S}_{00}^{\text{opt}}$ for the point target case, which is generally not needed for randomly generated channels.

B. Semi-Closed-Form Solution to Problem (P2) in Special Case with Low SNR

To gain more insights, this subsection further considers the special case with low communication SNR (i.e., $\frac{P}{\sigma_{\text{ID}}^2} \text{tr}(\mathbf{H}_{\text{ID}}^H \mathbf{H}_{\text{ID}}) \rightarrow 0$), and obtains a structured solution to problem (P2) in this case. Towards this end, we transform problem (P2) as problem (P2.3) similarly as in Section V-A, and then focus on solving (P2.3). In (P2.3), maximizing $\log_2 \det \left(\mathbf{I}_{N_{\text{ID}}} + \frac{1}{\sigma_{\text{ID}}^2} \widetilde{\mathbf{H}}_{\text{ID}} \mathbf{S}_1 \widetilde{\mathbf{H}}_{\text{ID}}^H \right)$ is equivalent to maximizing $\text{tr}(\widetilde{\mathbf{H}}_{\text{ID}} \mathbf{S}_1 \widetilde{\mathbf{H}}_{\text{ID}}^H)$ due to the low SNR consideration. Accordingly, (P2.3) is reformulated as

$$(\text{P3}) : \max_{\mathbf{S}_1 \succeq \mathbf{0}, p_0 \geq 0} \text{tr}(\widetilde{\mathbf{H}}_{\text{ID}} \mathbf{S}_1 \widetilde{\mathbf{H}}_{\text{ID}}^H) \quad (34a)$$

$$\text{s.t. } \text{tr}(\widetilde{\mathbf{H}}_{\text{EH}} \mathbf{S}_1 \widetilde{\mathbf{H}}_{\text{EH}}^H) \geq \Gamma_{\text{EH}} \quad (34b)$$

$$\text{tr}(\mathbf{S}_1^{-1}) + (M - r) \frac{1}{p_0} \leq \Gamma_{\text{S},2} \quad (34c)$$

$$\text{tr}(\mathbf{S}_1) + (M - r)p_0 \leq P. \quad (34d)$$

Proposition 5: The semi-closed-form optimal solution to problem (P3) is given by

$$\mathbf{S}_1^{\text{low}} = \mathbf{Q}_{\text{e}} \text{diag} \left(\sqrt{\frac{\mu^*}{\sigma_{\text{e},1}}}, \dots, \sqrt{\frac{\mu^*}{\sigma_{\text{e},r}}} \right) \mathbf{Q}_{\text{e}}^H, \quad (35)$$

$$p_0^{\text{low}} = \sqrt{\frac{\mu^*}{\nu^*}}, \quad (36)$$

where $\lambda^* \geq 0$, $\mu^* > 0$, and $\nu^* > 0$ denote the optimal dual variables associated with the constraints in (34b), (34c), and (34d) in (P3), respectively, and \mathbf{Q}_{e} and $\{\sigma_{\text{e},k}\}, \forall k \in \{1, \dots, r\}$, are obtained based on the EVD $\nu^* \mathbf{I}_r - \widetilde{\mathbf{H}}_{\text{ID}}^H \widetilde{\mathbf{H}}_{\text{ID}} - \lambda^* \widetilde{\mathbf{H}}_{\text{EH}}^H \widetilde{\mathbf{H}}_{\text{EH}} = \mathbf{Q}_{\text{e}} \text{diag}(\sigma_{\text{e},1}, \dots, \sigma_{\text{e},r}) \mathbf{Q}_{\text{e}}^H$.

Proof: See Appendix D.

Based on Proposition 5 and (33), we obtain the optimal transmit covariance solution in the low SNR case as $\mathbf{S}^{\text{low}} = \mathbf{V}^{\text{null}} \mathbf{S}_1^{\text{low}} \mathbf{V}^{\text{null}H} + p_0^{\text{low}} \mathbf{V}^{\text{null}} \mathbf{V}^{\text{null}H}$, which is also of full rank.

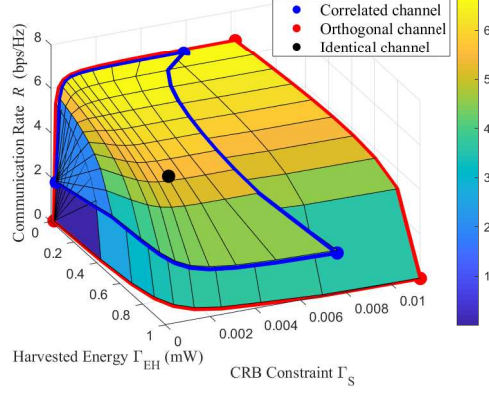


Fig. 3. The Pareto boundary of the C-R-E region for the point target case with $N_{\text{ID}} = N_{\text{EH}} = 1$ and $P = 50$ dBm.

It is observed in (35) that $\mathbf{S}_1^{\text{low}}$ is obtained following the EMT structure based on matrix $\nu^* \mathbf{I}_r - \widetilde{\mathbf{H}}_{\text{ID}}^H \widetilde{\mathbf{H}}_{\text{ID}} - \lambda^* \widetilde{\mathbf{H}}_{\text{EH}}^H \widetilde{\mathbf{H}}_{\text{EH}}$, together with a channel-inversion-like power allocation, with $\{\sigma_{e,k}\}, \forall k \in \{1, \dots, r\}$, denoting the equivalent channel power gains.

VI. NUMERICAL RESULTS

This section evaluates the performance of our proposed optimal designs. In the simulation, the H-AP is equipped with a ULA of $M = 10$ and $N_s = 16$ antennas with half-wavelength spacing between consecutive antennas. The target angle is $\theta = \frac{\pi}{3}$, and the reflection coefficient is set as $\alpha = 10^{-8}$, accounting for a round-trip path loss of 160 dB. The ID channel and the EH channel are set as $\mathbf{H}_{\text{ID}} = \alpha_{\text{ID}} \widehat{\mathbf{H}}_{\text{ID}}$ and $\mathbf{H}_{\text{EH}} = \alpha_{\text{EH}} \widehat{\mathbf{H}}_{\text{EH}}$, where α_{ID}^2 and α_{EH}^2 correspond to the path loss of 120 dB and 60 dB, respectively, and $\widehat{\mathbf{H}}_{\text{ID}}$ and $\widehat{\mathbf{H}}_{\text{EH}}$ correspond to the normalized channel accounting for the small-scale fading. The transmission duration is set as $L = 256$. The noise powers at the sensing receiver and the ID receiver are set to be $\sigma_s^2 = \sigma_{\text{ID}}^2 = -80$ dBm.

Fig. 3 shows the Pareto boundary of the C-R-E region for the point target case with $N_{\text{ID}} = N_{\text{EH}} = 1$, $P = 50$ dBm, and target angle $\theta = 0$. In this figure, we consider the line-of-sight (LoS) channels for the ID and EH channels, i.e., $\widehat{\mathbf{H}}_{\text{ID}} = \mathbf{a}_t^T(\theta_{\text{ID}})$ and $\widehat{\mathbf{H}}_{\text{EH}} = \mathbf{a}_t^T(\theta_{\text{EH}})$, where $\sin \theta_{\text{ID}} = \frac{2\gamma}{M}$ and $\sin \theta_{\text{EH}} = \frac{4\gamma}{M}$ correspond to the angles of the ID and EH receivers, with γ being a parameter characterizing the correlations among \mathbf{H}_s , \mathbf{H}_{ID} , and \mathbf{H}_{EH} . In particular, we consider three cases with $\gamma = 0, 0.4$, and 1, which correspond to the cases when the sensing, ID, and EH channels are identical, correlated, and orthogonal, respectively. It is observed that for the identical channels with $\gamma = 0$, the Pareto boundary is a point, which means that the R-max, E-max, and C-min strategies are identical, and thus the three performance metrics are optimized at the same time. It is also observed that for the orthogonal channels with $\gamma = 1$, optimizing one

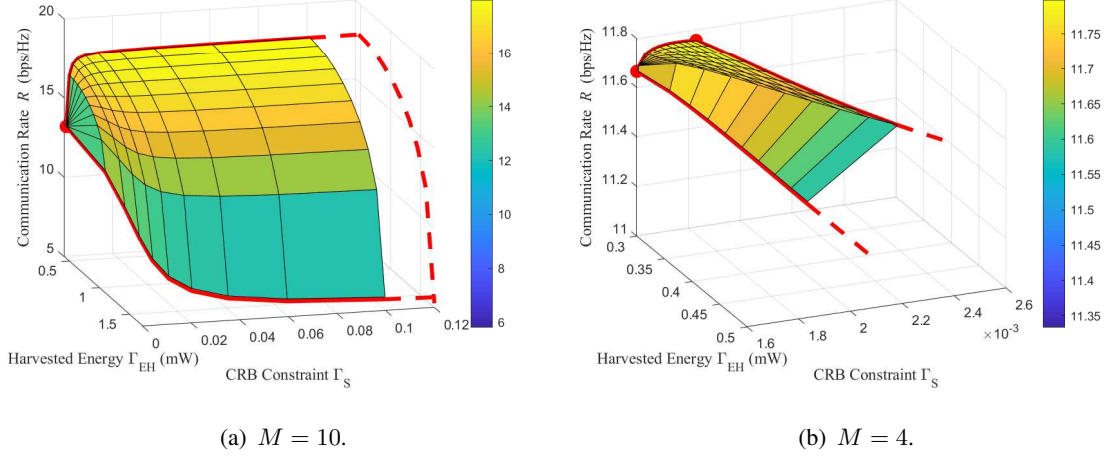


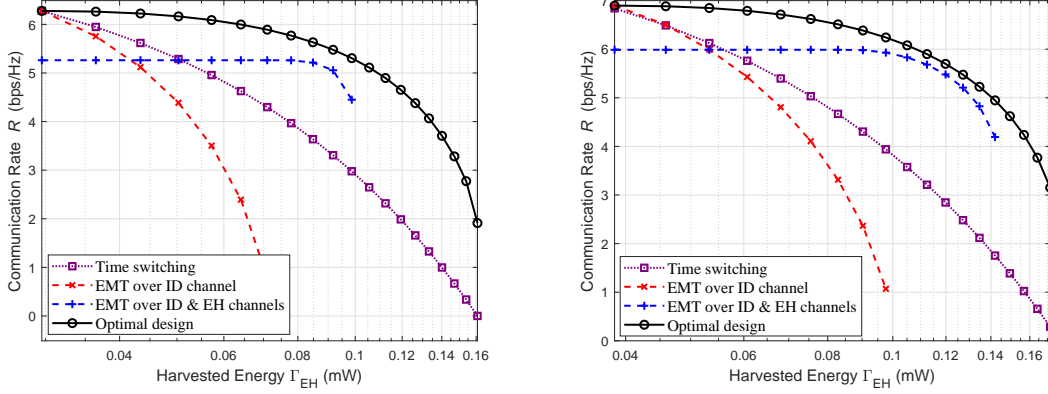
Fig. 4. The Pareto boundary of the C-R-E region for the extended target case with $N_{ID} = N_{EH} = 4$ and $P = 50$ dBm.

metric (e.g., E-max) leads to poor performances for the other two (e.g., zero rate and highest CRB), thus showing that the three objectives are competing in this case. Furthermore, for the correlated channels with $\gamma = 0.4$, the C-R-E region boundary is observed to lie between those with $\gamma = 1$ and $\gamma = 0$, thus showing the C-R-E tradeoff in this case.

Figs. 4(a) and 4(b) show the Pareto boundaries of the C-R-E regions for the extended target case with $M = 10$ and $M = 4$, respectively, where $P = 50$ dBm and $N_{ID} = N_{EH} = 4$. We consider Rayleigh fading for the ID and EH channels, where $\widehat{\mathbf{H}}_{ID}$ and $\widehat{\mathbf{H}}_{EH}$ are generated as CSCG random matrices with each element being zero mean and unit variance. It is observed in Fig. 4(a) that when $M = 10$, the R-max vertex, the E-max vertex, and the R-E tradeoff edge are not achievable. This is due to the fact that $\text{CRB}_{ID,2} \rightarrow \infty$ and $\text{CRB}_{EH,2} \rightarrow \infty$ when $M > N_{ID} > 1$ (see Section III-A). When the CRB value Γ_S becomes large, the C-R-E region boundary surface is observed to be parallel to the CRB-axis. This is because in this case, the CRB constraint in (P2) can be easily satisfied, and thus will not affect the C-R tradeoff. Next, it is observed in Fig. 4(b) that when $M = N_{ID} = 4$, the R-max vertex is achieved and only the E-max vertex is not achievable. This is due to the fact that $\text{CRB}_{ID,2}$ is finite as \mathbf{S}_{ID} is of full rank, but $\text{CRB}_{EH,2} \rightarrow \infty$ as $M > 1$.

Next, we evaluate the performance of our proposed designs as compared to the following benchmark schemes based on time switching and EMT.

- **Time switching:** The transmission duration is divided into three portions, $t_{ID} \geq 0$, $t_{EH} \geq 0$, and $t_S \geq 0$, with $t_{ID} + t_{EH} + t_S = 1$, during which the H-AP employs the transmit covariance matrices \mathbf{S}_{ID} , \mathbf{S}_{EH} , and $\mathbf{S}_{S,i}$, respectively. For case $i \in (1, 2)$, the cor-



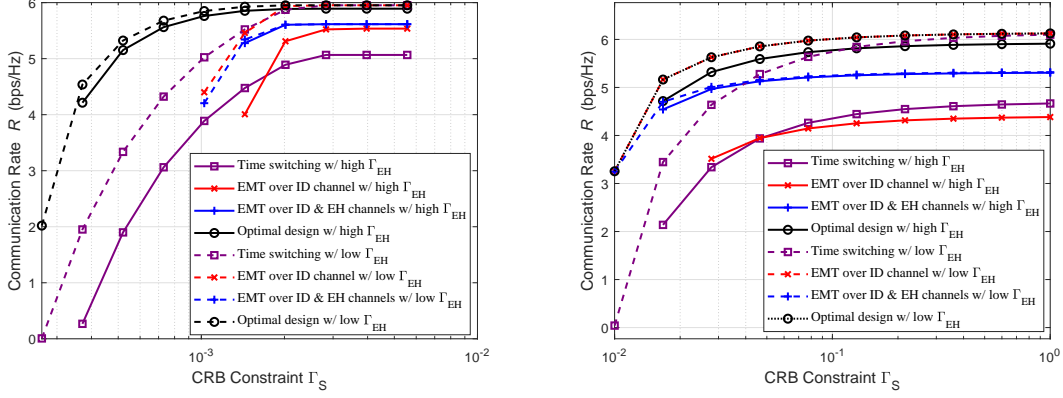
(a) Point target case.

(b) Extended target case.

Fig. 5. The communication rate R versus the energy constraint Γ_{EH} with $N_{ID} = N_{EH} = 4$ and $P = 40$ dBm.

responding communication rate, harvested energy, and estimation CRB are expressed as $R_{TS}(t_{ID}, t_{EH}, t_S) = t_{ID}R(\mathbf{S}_{ID})$, $E_{TS,i}(t_{ID}, t_{EH}, t_S) = t_{ID}E(\mathbf{S}_{ID}) + t_{EH}E(\mathbf{S}_{EH}) + t_SE(\mathbf{S}_{S,i})$, and $CRB_{TS,i}(t_{ID}, t_{EH}, t_S) = CRB_i(t_{ID}\mathbf{S}_{ID} + t_{EH}\mathbf{S}_{EH} + t_S\mathbf{S}_{S,i})$, respectively. The time portions t_{ID} , t_{EH} , and t_S are optimized to achieve different C-R-E tradeoffs.

- **EMT over ID channel:** This scheme is motivated by the communication-optimal EMT design for MIMO communication. For the point target case, supposing that the SVD of the ID channel \mathbf{H}_{ID} is $\mathbf{H}_{ID} = \mathbf{U}_{ID}\mathbf{\Lambda}_{ID}\mathbf{V}_{ID}^H$, we design the transmit covariance as $\mathbf{S} = \mathbf{V}_{ID}\hat{\mathbf{S}}^{ID}\mathbf{V}_{ID}^H$, where $\hat{\mathbf{S}}^{ID}$ is a diagonal matrix that is optimized based on problem (P1). For the extended target case, supposing the SVD of the projected ID channel $\tilde{\mathbf{H}}_{ID}$ in problem (P2.2) is $\tilde{\mathbf{H}}_{ID} = \tilde{\mathbf{U}}_{ID}\tilde{\mathbf{\Lambda}}_{ID}\tilde{\mathbf{V}}_{ID}^H$, we design the transmit covariance as $\mathbf{S} = \mathbf{V}^{\text{null}}\mathbf{S}_1\mathbf{V}^{\text{null}H} + p_0\mathbf{V}^{\text{null}}\mathbf{V}^{\text{null}H} = \mathbf{V}^{\text{null}}\tilde{\mathbf{V}}_{ID}\hat{\mathbf{S}}_1^{ID}\tilde{\mathbf{V}}_{ID}^H\mathbf{V}^{\text{null}H} + p_0\mathbf{V}^{\text{null}}\mathbf{V}^{\text{null}H}$ based on (33), where $\hat{\mathbf{S}}_1^{ID}$ is a diagonal matrix that is optimized together with p_0 based on problem (P2.3).
- **EMT over combined ID and EH channels:** This scheme is motivated by the optimal solution to (P2), in which the SVD of the combined ID and EH channels $\mathbf{H} = [\mathbf{H}_{ID}^T \mathbf{H}_{EH}^T]^T$ is employed to facilitate the optimization. As a result, for the point target case, supposing that the SVD of \mathbf{H} is $\mathbf{H} = \mathbf{U}\mathbf{\Lambda}\mathbf{V}^H$, we design the transmit covariance as $\mathbf{S} = \mathbf{V}\hat{\mathbf{S}}\mathbf{V}^H$, where $\hat{\mathbf{S}}$ is a diagonal matrix that is optimized based on problem (P1). For the extended target case, supposing the SVD of the combined projected ID and EH channels $\tilde{\mathbf{H}} = [\tilde{\mathbf{H}}_{ID}^T \tilde{\mathbf{H}}_{EH}^T]^T$ is $\tilde{\mathbf{H}} = \tilde{\mathbf{U}}\tilde{\mathbf{\Lambda}}\tilde{\mathbf{V}}^H$, we design the transmit covariance as $\mathbf{S} = \mathbf{V}^{\text{null}}\mathbf{S}_1\mathbf{V}^{\text{null}H} + p_0\mathbf{V}^{\text{null}}\mathbf{V}^{\text{null}H} = \mathbf{V}^{\text{null}}\tilde{\mathbf{V}}\hat{\mathbf{S}}_1\tilde{\mathbf{V}}^H\mathbf{V}^{\text{null}H} + p_0\mathbf{V}^{\text{null}}\mathbf{V}^{\text{null}H}$ based on (33), where $\hat{\mathbf{S}}_1$ is a diagonal matrix that is optimized together with p_0 based on problem (P2.3).



(a) Point target case.

(b) Extended target case.

Fig. 6. The communication rate R versus the CRB constraint Γ_S with $N_{ID} = N_{EH} = 4$ and $P = 40$ dBm.

Figs. 5(a) and 5(b) show the obtained communication rate R by problems (P1) and (P2) versus the EH constraint Γ_{EH} for the point and extended target cases, where the sensing constraints are set as $\Gamma_S = 50\text{CRB}_{\min,1}$ and $\Gamma_S = 50\text{CRB}_{\min,2}$, respectively. Here, we set $P = 40$ dBm and $N_{ID} = N_{EH} = 4$, and consider Rayleigh fading for $\widehat{\mathbf{H}}_{ID}$ and $\widehat{\mathbf{H}}_{EH}$. It is observed that for each target case, our proposed optimal design outperforms the other three benchmark schemes, and the performance gap becomes more significant when Γ_{EH} becomes large. Next, the EMT over combined ID and EH channels is observed to outperform the time switching and the EMT over ID channel in the medium regime of Γ_{EH} . This shows the benefit of considering both ID and EH channels for EMT in this case. In addition, the time switching and the EMT over ID channel are observed to perform close to the proposed optimal design when Γ_{EH} is low. This is because the three schemes become identical to the communication-optimal design in this case, as both the CRB constraint and the EH constraint become loose.

Figs. 6(a) and 6(b) show the obtained communication rate R by problems (P1) and (P2) versus the estimation CRB constraint Γ_S for the point and extended target cases, respectively, in which two EH constraints $\Gamma_{EH} = 0.5E_{\max}$ (high Γ_{EH} case) and $\Gamma_{EH} = 0.05E_{\max}$ (low Γ_{EH} case) are considered, with $P = 40$ dBm and $N_{ID} = N_{EH} = 4$. It is observed that for each case with different EH constraints, our proposed optimal design outperforms the other three benchmark schemes. Next, it is observed that the EMT over combined ID and EH channels outperforms the EMT over ID channel with high Γ_{EH} , and the opposite is true with low Γ_{EH} . This can be similarly explained as that for Figs. 5(a) and 5(b). Furthermore, with low Γ_{EH} , the time switching and the EMT over ID channel are observed to perform close to the optimal design when Γ_S

becomes large. This is due to the fact that both schemes can achieve the R-max vertex with the maximum communication rate in this case.

VII. CONCLUSION

This paper studied the fundamental C-R-E performance limits for a new multi-functional MIMO system integrating triple functions of sensing, communication, and powering. For both the point and extended target cases, we characterized the Pareto boundaries of the so-called C-R-E regions, by optimally solving new MIMO communication rate maximization problems subject to both EH and estimation CRB constraints. It was shown that for the point target case, the resultant C-R-E tradeoff highly depends on the correlations of the ID, EH, and sensing channels; while for the extended target case, the resultant C-R-E tradeoff relies on the system configuration such as the number of antennas at the BS. Furthermore, the proposed optimal design was shown to significantly outperform the benchmark schemes based on time switching and EMT. It is our hope that this paper can pave a new avenue for utilizing radio signals for multiple purposes towards 6G.

APPENDIX

A. Proof of Proposition 1

Substituting (20) and (21), problem (19) is re-expressed as

$$\begin{aligned} \max_{\mathbf{S}_{11}, \mathbf{C}, \mathbf{S}_{00}} \quad & \log_2 \det \left(\mathbf{I}_{N_{\text{ID}}} + \frac{1}{\sigma_{\text{ID}}^2} \mathbf{H}_{\text{ID}} (\mathbf{Q}^{\overline{\text{null}}} \mathbf{S}_{11} \mathbf{Q}^{\overline{\text{null}H}} + \mathbf{Q}^{\overline{\text{null}}} \mathbf{C} \mathbf{Q}^{\text{null}H} + \mathbf{Q}^{\text{null}} \mathbf{C}^H \mathbf{Q}^{\overline{\text{null}H}} \right. \\ & \left. + \mathbf{Q}^{\text{null}} \mathbf{S}_{00} \mathbf{Q}^{\text{null}H}) \mathbf{H}_{\text{ID}}^H \right) - \text{tr}(\Sigma^{\overline{\text{null}}} \mathbf{S}_{11}), \\ \text{s.t.} \quad & \begin{bmatrix} \mathbf{S}_{11} & \mathbf{C} \\ \mathbf{C}^H & \mathbf{S}_{00} \end{bmatrix} \succeq \mathbf{0}. \end{aligned} \quad (37)$$

According to Lemma 1, to solve (19), we only need to deal with problem (37) for the case with $\mathbf{H}_{\text{ID}} (\mathbf{Q}^{\overline{\text{null}}} \mathbf{C} \mathbf{Q}^{\text{null}H} + \mathbf{Q}^{\text{null}} \mathbf{C}^H \mathbf{Q}^{\overline{\text{null}H}} + \mathbf{Q}^{\text{null}} \mathbf{S}_{00} \mathbf{Q}^{\text{null}H}) \mathbf{H}_{\text{ID}}^H = \mathbf{0}$. Therefore, we can simply choose $\mathbf{C}^* = \mathbf{0}$ and $\mathbf{S}_{00}^* = \mathbf{0}$ as the optimal solution of \mathbf{C} and \mathbf{S}_{00} for obtaining the dual function $g(\lambda, \nu, \mathbf{Z})$ only, and thus (37) is simplified as the optimization of \mathbf{S}_{11} in the following.

$$\max_{\mathbf{S}_{11} \succeq \mathbf{0}} \log_2 \det \left(\mathbf{I}_{N_{\text{ID}}} + \frac{1}{\sigma_{\text{ID}}^2} \mathbf{H}_{\text{ID}} \mathbf{Q}^{\overline{\text{null}}} \mathbf{S}_{11} \mathbf{Q}^{\overline{\text{null}H}} \mathbf{H}_{\text{ID}}^H \right) - \text{tr}(\Sigma^{\overline{\text{null}}} \mathbf{S}_{11}). \quad (38)$$

Define $\mathbf{S}_{11} = (\Sigma^{\overline{\text{null}}})^{-\frac{1}{2}} \mathbf{V}_p \tilde{\mathbf{S}}_{11} \mathbf{V}_p^H (\Sigma^{\overline{\text{null}}})^{-\frac{1}{2}}$. Problem (38) is re-expressed as

$$\max_{\tilde{\mathbf{S}}_{11} \succeq \mathbf{0}} \log_2 \det \left(\mathbf{I}_{r_p} + \frac{1}{\sigma_{\text{ID}}^2} \Lambda_p^H \Lambda_p \tilde{\mathbf{S}}_{11} \right) - \text{tr}(\tilde{\mathbf{S}}_{11}). \quad (39)$$

As shown in [8], the optimal solution to problem (39) is given by $\tilde{\mathbf{S}}_{11}^* = \text{diag}(\tilde{p}_1, \dots, \tilde{p}_{\tilde{r}_p})$, where $\tilde{p}_k = (\frac{1}{\ln 2} - \frac{\sigma_{\text{ID}}^2}{\lambda_{p,k}^2})^+$, $\forall k \in \{1, \dots, \tilde{r}_p\}$. Thus, the optimal solution of \mathbf{S}_{11} to (37) is

$$\mathbf{S}_{11}^* = (\Sigma^{\text{null}})^{-\frac{1}{2}} \mathbf{V}_p \tilde{\mathbf{S}}_{11}^* \mathbf{V}_p^H (\Sigma^{\text{null}})^{-\frac{1}{2}}. \quad (40)$$

B. Proof of Proposition 3

To facilitate the proof of this proposition, we first present the following lemma.

Lemma 2: Suppose that $\begin{bmatrix} \mathbf{S}_1 & \mathbf{B} \\ \mathbf{B}^H & \mathbf{S}_0 \end{bmatrix} \succeq \mathbf{0}$. It follows that

$$\text{tr} \left(\begin{bmatrix} \mathbf{S}_1 & \mathbf{B} \\ \mathbf{B}^H & \mathbf{S}_0 \end{bmatrix}^{-1} \right) \geq \text{tr} \left(\begin{bmatrix} \mathbf{S}_1 & \mathbf{0} \\ \mathbf{0} & \mathbf{S}_0 \end{bmatrix}^{-1} \right). \quad (41)$$

Proof: Based on the Schur complement, it follows that $\begin{bmatrix} \mathbf{S}_1 & \mathbf{B} \\ \mathbf{B}^H & \mathbf{S}_0 \end{bmatrix} \succeq \mathbf{0}$ is equivalent to $\mathbf{S}_1 \succeq \mathbf{0}$ and $\mathbf{F}_1 = \mathbf{S}_0 - \mathbf{B}^H \mathbf{S}_1^{-1} \mathbf{B} \succeq \mathbf{0}$. Similarly, $\begin{bmatrix} \mathbf{S}_1 & \mathbf{B} \\ \mathbf{B}^H & \mathbf{S}_0 \end{bmatrix} \succeq \mathbf{0}$ is also equivalent to $\mathbf{S}_0 \succeq \mathbf{0}$ and $\mathbf{F}_0 = \mathbf{S}_1 - \mathbf{B} \mathbf{S}_0^{-1} \mathbf{B}^H \succeq \mathbf{0}$. According to the partitioned matrix formula, we have

$$\begin{bmatrix} \mathbf{S}_1 & \mathbf{B} \\ \mathbf{B}^H & \mathbf{S}_0 \end{bmatrix}^{-1} = \begin{bmatrix} \mathbf{F}_0^{-1} & -\mathbf{S}_1^{-1} \mathbf{B} \mathbf{F}_1^{-1} \\ -\mathbf{F}_1^{-1} \mathbf{B}^H \mathbf{S}_1^{-1} & \mathbf{F}_1^{-1} \end{bmatrix}, \quad (42)$$

$$\begin{bmatrix} \mathbf{S}_1 & \mathbf{0} \\ \mathbf{0}^H & \mathbf{S}_0 \end{bmatrix}^{-1} = \begin{bmatrix} \mathbf{S}_1^{-1} & \mathbf{0} \\ \mathbf{0} & \mathbf{S}_0^{-1} \end{bmatrix}. \quad (43)$$

Since $\mathbf{F}_1 \succeq \mathbf{0}$ and $\mathbf{F}_0 \succeq \mathbf{0}$, we have $\text{tr}(\mathbf{F}_0^{-1}) = \text{tr}(\mathbf{S}_1^{-1} + \mathbf{S}_1^{-1} \mathbf{B} \mathbf{F}_1^{-1} \mathbf{B}^H \mathbf{S}_1^{-1}) \geq \text{tr}(\mathbf{S}_1^{-1})$ and $\text{tr}(\mathbf{F}_1^{-1}) = \text{tr}(\mathbf{S}_0^{-1} + \mathbf{S}_0^{-1} \mathbf{B}^H \mathbf{F}_0^{-1} \mathbf{B} \mathbf{S}_0^{-1}) \geq \text{tr}(\mathbf{S}_0^{-1})$, respectively. Therefore, it follows that

$$\text{tr} \left(\begin{bmatrix} \mathbf{S}_1 & \mathbf{B} \\ \mathbf{B}^H & \mathbf{S}_0 \end{bmatrix}^{-1} \right) = \text{tr}(\mathbf{F}_0^{-1}) + \text{tr}(\mathbf{F}_1^{-1}) \geq \text{tr}(\mathbf{S}_1^{-1}) + \text{tr}(\mathbf{S}_0^{-1}) = \text{tr} \left(\begin{bmatrix} \mathbf{S}_1 & \mathbf{0} \\ \mathbf{0} & \mathbf{S}_0 \end{bmatrix}^{-1} \right), \quad (44)$$

where the equality holds when $\mathbf{B} = \mathbf{0}$.

According to Lemma 2, it follows that subject to the constraint in (30e), the left-hand-side (LHS) of (30c) is minimized when $\mathbf{B} = \mathbf{0}$. Therefore, Proposition 3 is proved.

C. Proof of Proposition 4

To facilitate the proof, we first present the following lemma.

Lemma 3: Suppose that $\mathbf{S}_0 \in \mathbb{S}_+^{M-r}$ with diagonal elements $p_{0,1}, \dots, p_{0,M-r}$. It follows that

$$\text{tr}(\mathbf{S}_0^{-1}) \geq \text{tr}(\text{diag}(p_{0,1}, \dots, p_{0,M-r})^{-1}), \quad (45)$$

where $p_{0,k} \geq 0, \forall k \in \{1, \dots, M-r\}$.

Proof: First, we decompose \mathbf{S}_0 as

$$\mathbf{S}_0 = \begin{bmatrix} \mathbf{S}_{0,1} & \mathbf{s}_{0,1} \\ \mathbf{s}_{0,1}^H & p_{0,M-r} \end{bmatrix}, \quad (46)$$

where $\mathbf{S}_{0,1} \in \mathbb{S}^{M-r-1}$ and $\mathbf{s}_{0,1} \in \mathbb{C}^{(M-r-1) \times 1}$. According to Lemma 2 in Appendix B, we have

$$\text{tr} \left(\begin{bmatrix} \mathbf{S}_{0,1} & \mathbf{s}_{0,1} \\ \mathbf{s}_{0,1}^H & p_{0,M-r} \end{bmatrix}^{-1} \right) \geq \text{tr} \left(\begin{bmatrix} \mathbf{S}_{0,1} & \mathbf{0} \\ \mathbf{0} & p_{0,M-r} \end{bmatrix}^{-1} \right), \quad (47)$$

where $\mathbf{S}_{0,1} \succeq \mathbf{0}$ and $p_{0,M-r} \geq 0$. Then, we further decompose $\mathbf{S}_{0,1}$ to $\mathbf{S}_{0,2} \in \mathbb{S}^{M-r-2}, \dots, \mathbf{S}_{0,M-r-1} = p_{0,1}$. After repeating the argument above, this lemma can be proved.

We assume that \mathbf{S}_0 is not diagonal, whose diagonal elements are $p_{0,k} \geq 0, \forall k \in \{1, \dots, M-r\}$. Let $p_0 \triangleq \frac{\sum_{k=1}^{M-r} p_{0,k}}{M-r}$. According to Lemma 3, we have $\text{tr}(\mathbf{S}_0^{-1}) \geq \text{tr}(\text{diag}(p_{0,1}, \dots, p_{0,M-r})^{-1}) = \sum_{k=1}^{M-r} \frac{1}{p_{0,k}} \geq \frac{M-r}{p_0} = \text{tr}((p_0 \mathbf{I}_{M-r})^{-1})$, where the second inequality holds based on the harmonic inequality. Thus, subject to the constraints in (31d) and (31e), the LHS of (31c) is minimized by removing the non-diagonal elements of \mathbf{S}_0 and averaging its diagonal elements. Therefore, Proposition 4 is proved.

D. Proof of Proposition 5

Let $\lambda \geq 0$, $\mu \geq 0$, and $\nu \geq 0$ denote the dual variables associated with the constraints in (34b), (34c), and (34d), respectively. The Lagrangian of problem (P3) is given by

$$\begin{aligned} \mathcal{L}_3(\mathbf{S}_1, p_0, \lambda, \mu, \nu) &= \text{tr}(\widetilde{\mathbf{H}}_{\text{ID}} \mathbf{S}_1 \widetilde{\mathbf{H}}_{\text{ID}}^H) + \lambda (\text{tr}(\widetilde{\mathbf{H}}_{\text{EH}} \mathbf{S}_1 \widetilde{\mathbf{H}}_{\text{EH}}^H) - \Gamma_{\text{EH}}) \\ &\quad + \mu (\Gamma_{\text{S},2} - \text{tr}(\mathbf{S}_1^{-1}) - (M-r) \frac{1}{p_0}) + \nu (P - \text{tr}(\mathbf{S}_1) - (M-r)p_0) \\ &= -\text{tr}(\mathbf{E} \mathbf{S}_1) - \mu \text{tr}(\mathbf{S}_1^{-1}) - (M-r) \left(\frac{\mu}{p_0} + \nu p_0 \right) - \lambda \Gamma_{\text{EH}} + \mu \Gamma_{\text{S},2} + \nu P, \end{aligned} \quad (48)$$

where $\mathbf{E} \triangleq \nu \mathbf{I}_r - \widetilde{\mathbf{H}}_{\text{ID}}^H \widetilde{\mathbf{H}}_{\text{ID}} - \lambda \widetilde{\mathbf{H}}_{\text{EH}}^H \widetilde{\mathbf{H}}_{\text{EH}}$. Accordingly, the dual function of (P3) is defined as

$$g_3(\lambda, \mu, \nu) = \max_{\mathbf{S}_1 \succeq \mathbf{0}, p_0 \geq 0} \mathcal{L}_3(\mathbf{S}_1, p_0, \lambda, \mu, \nu). \quad (49)$$

We have the following lemma, which can be verified similarly as Lemma 1.

Lemma 4: In order for the dual function $g_3(\lambda, \mu, \nu)$ to be bounded from above, it must hold that $\mathbf{E} \succeq \mathbf{0}$.

Based on Lemma 4, the dual problem of (P3) is defined as

$$(D3) : \min_{\lambda \geq 0, \mu \geq 0, \nu \geq 0} g_3(\lambda, \mu, \nu), \text{ s.t. } \mathbf{E} \succeq \mathbf{0}. \quad (50)$$

Since (P3) is convex and satisfies the Slater's condition, strong duality holds between (P3) and its dual problem (D3) [30]. Therefore, we can solve (P3) by equivalently solving (D3).

First, we find the dual function $g_3(\lambda, \mu, \nu)$ in (49) under given $\lambda \geq 0$, $\mu \geq 0$, and $\nu \geq 0$. By dropping the constant terms $-\lambda\Gamma_{\text{EH}} + \mu\Gamma_{\text{S},2} + \nu P$, the problem in (49) is equivalent to

$$\max_{\mathbf{S}_1 \succeq \mathbf{0}, p_0 \geq 0} -\text{tr}(\mathbf{E}\mathbf{S}_1) - \mu\text{tr}(\mathbf{S}_1^{-1}) - (M-r)\left(\frac{\mu}{p_0} + \nu p_0\right). \quad (51)$$

The EVD of \mathbf{E} is expressed as $\mathbf{E} = \mathbf{Q}_e \Sigma_e \mathbf{Q}_e^H$, where $\Sigma_e = \text{diag}(\sigma_{e,1}, \dots, \sigma_{e,r})$. Without loss of generality, we assume $\sigma_{e,1} \geq \dots \geq \sigma_{e,r} \geq 0$. Define $\tilde{\mathbf{S}}_1 = \mathbf{Q}_e \tilde{\mathbf{S}}_1 \mathbf{Q}_e^H$. Problem (51) is re-expressed as

$$\max_{\tilde{\mathbf{S}}_1 \succeq \mathbf{0}, p_0 \geq 0} -\text{tr}(\Sigma_e \tilde{\mathbf{S}}_1) - \mu\text{tr}(\tilde{\mathbf{S}}_1^{-1}) - (M-r)\left(\frac{\mu}{p_0} + \nu p_0\right). \quad (52)$$

According to Lemma 3 in Appendix C, the optimal solution of $\tilde{\mathbf{S}}_1$ to problem (52) is diagonal, i.e., we have $\tilde{\mathbf{S}}_1 = \text{diag}(\tilde{p}_{1,1}, \dots, \tilde{p}_{1,r})$. Therefore, (52) is re-expressed as

$$\max_{\{\tilde{p}_{1,k} \geq 0\}, p_0 \geq 0} -\sum_{k=1}^r \left(\sigma_{e,k} \tilde{p}_{1,k} + \frac{\mu}{\tilde{p}_{1,k}} \right) - (M-r)\left(\frac{\mu}{p_0} + \nu p_0\right). \quad (53)$$

Notice that for the case with $\sigma_{e,r} = 0$, i.e., \mathbf{E} is rank-deficient, the optimality of problem (53) cannot be achieved unless $\mu = 0$. However, it is easy to verify that at the optimality of problem (P3), the constraints (34c) and (34d) should be tight. Therefore, it follows that $\mu > 0$ and $\nu > 0$, which means that we should have $\sigma_{e,r} > 0$, i.e., the dual problem (D3) should also satisfy the constraint $\mathbf{E} \succ \mathbf{0}$ to achieve the optimality.

By checking the first derivative, the optimal solution to problem (53) is

$$\tilde{p}_{1,k}^* = \sqrt{\frac{\mu}{\sigma_{e,k}}}, \forall k \in \{1, \dots, r\}, \quad (54)$$

$$p_0^* = \sqrt{\frac{\mu}{\nu}}. \quad (55)$$

Thus, the optimal solution of \mathbf{S}_1 to problem (51) is

$$\mathbf{S}_1^* = \mathbf{Q}_e \text{diag}(\tilde{p}_{1,1}^*, \dots, \tilde{p}_{1,r}^*) \mathbf{Q}_e^H. \quad (56)$$

Next, we solve the dual problem (D3), which is convex but not necessarily differentiable, and thus can be solved by applying the subgradient-based method such as the ellipsoid method. For the objective function $g_3(\lambda, \mu, \nu)$, the subgradient at (λ, μ, ν) is $\left[\text{tr}(\widetilde{\mathbf{H}}_{\text{EH}}^H \widetilde{\mathbf{H}}_{\text{EH}} \mathbf{S}_1^*) - \Gamma_{\text{EH}}, \Gamma_{\text{S},2} - \text{tr}((\mathbf{S}_1^*)^{-1}) - (M-r)\frac{1}{p_0^*}, P - \text{tr}(\mathbf{S}_1^*) - (M-r)p_0^* \right]^T$. Furthermore, let \mathbf{q}_3 denote the eigenvector of \mathbf{E} corresponding to its minimum eigenvalue $\sigma_{\text{e},r}$. With the similar analysis as in Section IV, the subgradient of constraint $\mathbf{E} \succ \mathbf{0}$ at (λ, μ, ν) is $[\mathbf{q}_3^H \widetilde{\mathbf{H}}_{\text{EH}}^H \widetilde{\mathbf{H}}_{\text{EH}} \mathbf{q}_3, 0, -1]^T$.

Finally, we present the optimal solution to the primal problem (P3). With the optimal dual variables λ^* , μ^* , and ν^* at hand, the corresponding optimal solutions \mathbf{S}_1^* and p_0^* in (56) and (55) to problem (51) can be directly used for constructing the optimal primal solutions to (P3), denoted by $\mathbf{S}_1^{\text{low}}$ and p_0^{low} , respectively. This thus completes the proof of this proposition.

REFERENCES

- [1] Y. Chen, H. Hua, and J. Xu, "Transmit optimization for multi-functional MIMO systems integrating sensing, communication, and powering," submitted to *IEEE ICC 2023*, *arXiv preprint arXiv:2210.16716*, 2022.
- [2] Y. Cui, F. Liu, X. Jing, and J. Mu, "Integrating sensing and communications for ubiquitous IoT: Applications, trends, and challenges," *IEEE Netw.*, vol. 35, no. 5, pp. 158–167, Sep. 2021.
- [3] W. Saad, M. Bennis, and M. Chen, "A vision of 6G wireless systems: Applications, trends, technologies, and open research problems," *IEEE Netw.*, vol. 34, no. 3, pp. 134–142, May 2020.
- [4] W. Tong and P. Zhu, *6G: The Next Horizon: From Connected People and Things to Connected Intelligence*. Cambridge University Press, 2021, pp. 24–26.
- [5] B. Clerckx, R. Zhang, R. Schober, D. W. K. Ng, D. I. Kim, and H. V. Poor, "Fundamentals of wireless information and power transfer: From RF energy harvester models to signal and system designs," *IEEE J. Sel. Areas Commun.*, vol. 37, no. 1, pp. 4–33, Jan. 2019.
- [6] Y. Zeng, B. Clerckx, and R. Zhang, "Communications and signals design for wireless power transmission," *IEEE Trans. Commun.*, vol. 65, no. 5, pp. 2264–2290, May 2017.
- [7] F. Liu, Y. Cui, C. Masouros, J. Xu, T. X. Han, Y. C. Eldar, and S. Buzzi, "Integrated sensing and communications: Toward dual-functional wireless networks for 6G and beyond," *IEEE J. Sel. Areas Commun.*, vol. 40, no. 6, pp. 1728–1767, Jun. 2022.
- [8] R. Zhang and C. K. Ho, "MIMO broadcasting for simultaneous wireless information and power transfer," *IEEE Trans. Wireless Commun.*, vol. 12, no. 5, pp. 1989–2001, May 2013.
- [9] J. Xu, L. Liu, and R. Zhang, "Multiuser MISO beamforming for simultaneous wireless information and power transfer," *IEEE Trans. Signal Process.*, vol. 62, no. 18, pp. 4798–4810, Sep. 2014.
- [10] S. Luo, J. Xu, T. J. Lim, and R. Zhang, "Capacity region of MISO broadcast channel for simultaneous wireless information and power transfer," *IEEE Trans. Commun.*, vol. 63, no. 10, pp. 3856–3868, Oct. 2015.
- [11] J. Park and B. Clerckx, "Joint wireless information and energy transfer in a two-user MIMO interference channel," *IEEE Trans. Wireless Commun.*, vol. 12, no. 8, pp. 4210–4221, Aug. 2013.
- [12] D. W. K. Ng, E. S. Lo, and R. Schober, "Robust beamforming for secure communication in systems with wireless information and power transfer," *IEEE Trans. Wireless Commun.*, vol. 13, no. 8, pp. 4599–4615, Aug. 2014.

- [13] E. Boshkovska, D. W. K. Ng, N. Zlatanov, and R. Schober, "Practical non-linear energy harvesting model and resource allocation for SWIPT systems," *IEEE Commun. Lett.*, vol. 19, no. 12, pp. 2082–2085, Dec. 2015.
- [14] Y. Xiong, F. Liu, Y. Cui, W. Yuan, and T. X. Han, "Flowing the information from Shannon to Fisher: Towards the fundamental tradeoff in ISAC," *arXiv preprint arXiv:2204.06938*, 2022.
- [15] H. Hua, T. X. Han, and J. Xu, "MIMO integrated sensing and communication: CRB-rate tradeoff," *arXiv preprint arXiv:2209.12721*, 2022.
- [16] F. Liu, C. Masouros, A. Li, H. Sun, and L. Hanzo, "MU-MIMO communications with MIMO radar: From co-existence to joint transmission," *IEEE Trans. Wireless Commun.*, vol. 17, no. 4, pp. 2755–2770, Apr. 2018.
- [17] X. Liu, T. Huang, N. Shlezinger, Y. Liu, J. Zhou, and Y. C. Eldar, "Joint transmit beamforming for multiuser MIMO communications and MIMO radar," *IEEE Trans. Signal Process.*, vol. 68, pp. 3929–3944, Jun. 2020.
- [18] H. Hua, J. Xu, and T. X. Han, "Optimal transmit beamforming for integrated sensing and communication," *arXiv preprint arXiv:2104.11871*, 2021.
- [19] J. A. Zhang, X. Huang, Y. J. Guo, J. Yuan, and R. W. Heath, "Multibeam for joint communication and radar sensing using steerable analog antenna arrays," *IEEE Trans. Veh. Technol.*, vol. 68, no. 1, pp. 671–685, Jan. 2019.
- [20] C. Xu, B. Clerckx, S. Chen, Y. Mao, and J. Zhang, "Rate-splitting multiple access for multi-antenna joint radar and communications," *IEEE J. Sel. Topics Signal Process.*, vol. 15, no. 6, pp. 1332–1347, Nov. 2021.
- [21] L. Yin, Y. Mao, O. Dizdar, and B. Clerckx, "Rate-splitting multiple access for 6G—part II: Interplay with integrated sensing and communications," *arXiv preprint arXiv:2205.02462*, 2022.
- [22] Z. Wang, Y. Liu, X. Mu, Z. Ding, and O. A. Dobre, "NOMA empowered integrated sensing and communication," *IEEE Commun. Lett.*, vol. 26, no. 3, pp. 677–681, Mar. 2022.
- [23] J. Li, L. Xu, P. Stoica, K. W. Forsythe, and D. W. Bliss, "Range compression and waveform optimization for MIMO radar: A Cramér-Rao bound based study," *IEEE Trans. Signal Process.*, vol. 56, no. 1, pp. 218–232, Jan. 2008.
- [24] I. Bekkerman and J. Tabrikian, "Target detection and localization using MIMO radars and sonars," *IEEE Trans. Signal Process.*, vol. 54, no. 10, pp. 3873–3883, Oct. 2006.
- [25] E. Telatar, "Capacity of multi-antenna Gaussian channels," *Eur. Trans. Telecommun.*, vol. 10, no. 6, pp. 585–595, Nov. 1999.
- [26] F. Liu, Y.-F. Liu, A. Li, C. Masouros, and Y. C. Eldar, "Cramér-Rao bound optimization for joint radar-communication beamforming," *IEEE Trans. Signal Process.*, vol. 70, pp. 240–253, Dec. 2021.
- [27] X. Song, J. Xu, F. Liu, T. X. Han, and Y. C. Eldar, "Intelligent reflecting surface enabled sensing: Cramér-Rao bound optimization," *arXiv preprint arXiv:2207.05611*, 2022.
- [28] M. Grant and S. Boyd, "CVX: Matlab software for disciplined convex programming, version 2.1," 2014.
- [29] Z. Ren, X. Song, Y. Fang, L. Qiu, and J. Xu, "Fundamental CRB-rate tradeoff in multi-antenna multicast channel with ISAC," *arXiv preprint arXiv:2205.15615*, 2022.
- [30] S. Boyd and L. Vandenberghe, *Convex Optimization*. Cambridge University Press, 2004.